5101-215
Flat-Plate
Solar Array Project

DOE/JPL-1012-85
Distribution Category UC-63b

FSA Field Test Report 1980-1982

H.G. Maxwell
C.A. Grimmett
J. Repar
P.O. Frickland
J.A. Amy

April 15, 1983

Prepared for
U.S. Department of Energy
Through an Agreement with
National Aeronautics and Space Administration
by
Jet Propulsion Laboratory
California Institute of Technology
Pasadena, California

JPL Publication 83-29

5101-215
Flat-Plate
Solar Array Project

DOE/JPL-1012-85
Distribution Category UC-63b

FSA Field Test Report 1980-1982

H.G. Maxwell
C.A. Grimmett
J. Repar
P.O. Frickland
J.A. Amy

April 15, 1983

Prepared for
U.S. Department of Energy
Through an Agreement with
National Aeronautics and Space Administration
by
Jet Propulsion Laboratory
California Institute of Technology
Pasadena, California

JPL Publication 83-29

Prepared by the Jet Propulsion Laboratory, California Institute of Technology, for the U.S. Department of Energy through an agreement with the National Aeronautics and Space Administration.

The JPL Flat-Plate Solar Array Project is sponsored by the U.S. Department of Energy and is part of the Photovoltaic Energy Systems Program to initiate a major effort toward the development of cost-competitive solar arrays.

This publication reports on work done under NASA Task RD-152, Amendment 66, DOE/NASA IAA No. DE-AI01-76ET20356.

ABSTRACT

Photovoltaic modules made of new and developing materials were tested in a continuing study of weatherability, compatibility, and corrosion protection. Over a two-year period, 365 two-cell submodules have been exposed for various intervals at three outdoor sites in Southern California or subjected to laboratory acceptance tests. Results to date show little loss of maximum power output, except in two types of modules. In the first of these, failure is due to cell fracture from the stresses that arise as water is regained from the surrounding air by a hardboard substrate, which shrank as it dried during its encapsulation in plastic film at 150°C *in vacuo*. In the second, the glass superstrate is sensitive to cracking, which also damages the cells electrostatically bonded to it; inadequate bonding of interconnects to the cells is also a problem in these modules. In a third type of module, a polyurethane pottant has begun to yellow, though as yet without significant effect on maximum power output.

ACKNOWLEDGMENTS

Module performance was evaluated at the JPL Flat-Plate Solar Array Project's Large-Area Pulsed Solar Simulator Facility, where testing was coordinated through John Griffith.

CONTENTS

Figures

Tables

SECTION I

INTRODUCTION

The minimodule and submodule field-testing program was initiated in 1980 as part of the Environmental Isolation Task of the Flat-Plate Solar Array Project (FSA). Its purpose is to provide information regarding the weatherability, compatibility, and corrosion protection of new and developing materials, using real-time outdoor exposure supplemented by a limited amount of accelerated testing. Observations of degradation modes and mechanisms resulting from such exposure can be combined with data from more extensive accelerated testing to define the phenomena that limit module life--knowledge crucial for developing accurate models to predict solar array performance.

This field-testing program made use of 150 minimodules of 11 Types--some quite similar in design--and 365 submodules (containing two cells) of four Types. Figure 1-1 provides a convenient guide to the important features of these module Types; more detailed information is presented in Section II and Appendix B. In brief, several modules of each Type were subjected to standard JPL qualification testing: thermal-cycle and humidity-freezing cycle tests, determination of nominal operating cell temperature (NOCT), partial-discharge test, and hail impact test. Some modules underwent accelerated testing at DSET Laboratories, Inc., Phoenix, Arizona. Most, however, were weathered at three locations in Southern California: JPL's main laboratory site in Pasadena, JPL's Goldstone Tracking Station in the Mojave Desert, and at a site just outside the U.S. Coast Guard Station at Pt. Vicente. Table 1-1 shows how these modules were distributed among the various tests.

All JPL qualification testing and DSET accelerated testing for this program have been completed. Minimodule and submodule field testing is a continuing effort that includes periodic visual, electrical, and chemical evaluation of the deployed modules. All modules that have failed during field testing (including those with zero power output) have been returned to their test sites after failure analysis so that additional materials degradation might occur.

ORIGINAL PAGE IS
OF POOR QUALITY

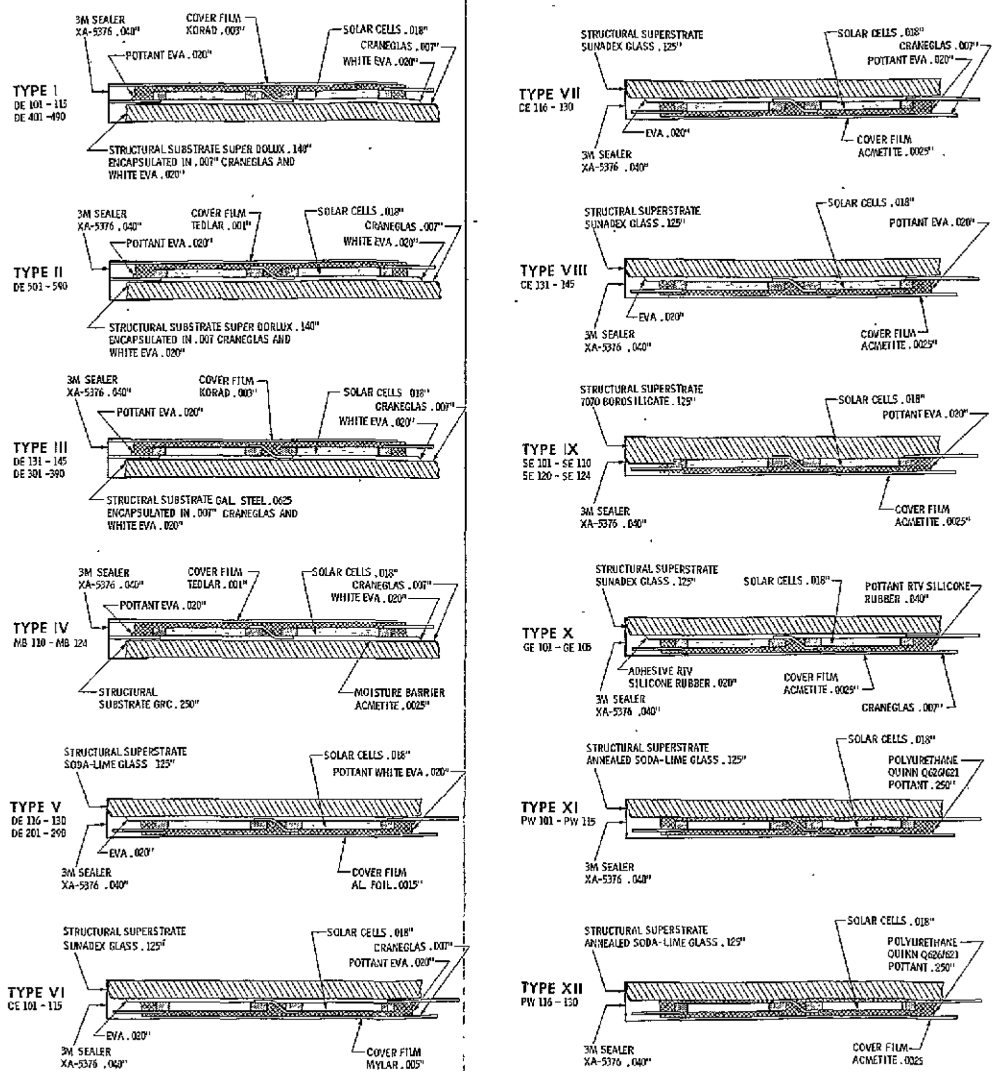

Figure 1-1. Module Types

FOLDOUT FRAME

ORIGINAL PAGE IS
OF POOR QUALITY

Table 1-1. Module Distribution

Module Type	Manufacturer	Serial Numbers	Number of Each Type	Envion-ment and Hail Test	Partial Discharge	Control	DSET	Outdoor Exposure		
								JPL	Gold-stone	Pt. Vicente
Mini-modules										
I	Springborn Laboratories	DE101-115	15	3	1	1	1	3	3	3
V		DE116-130	15	3	1	2	0	3	3	3
III		DE131-145	15	3	1	1	1	3	3	3
IV	MBAssociates	MB110-124	15	3	1	2	0	3	3	3
VI	Applied Solar Energy Corp.	CE101-115	15	3	1	2	0	3	3	3
VII		CE116-130	15	3	1	1	1	3	3	3
VIII		CE131-145	15	3	1	2	0	3	3	3
IX	Spire Corp.	SE101-110	10	1	1	1	1	2	2	2
		SE120-124	5	0	0	2	0	1	1	1
X	General Electric Company	GE101-105	5	1	1	0	0	1	1	1
XI	Photowatt Corp.	PW101-115	15	3	1	2	0	3	3	3
XII		PW116-130	15	3	1	2	0	3	3	3
Sub-modules										
V	Springborn Laboratories	DE201-290	90	0	0	19	6	23	21	21
III		DE301-390	90	0	0	20	6	23	21	20
I		DE401-490	90	0	0	18	6	23	20	23
II		DE501-590	90	0	0	19	6	23	21	21

FOLDOUT FRAME

SECTION II

MODULE DESIGNS AND MATERIALS

A. OVERVIEW

The field-testing program is intended to investigate both the degradation processes that occur in the materials of photovoltaic modules, and the resultant effects on electrical performance. It was not considered necessary to work with full-size commercial modules manufactured in a normal production run. Instead, smaller modules were produced in special laboratory runs, using designs and processes that could be used for manufacture of future full-size modules. For these reasons, it must be emphasized that the field test results cannot be applied directly to the rating of commercial products, although the results do provide insight into material response to common environmental stresses and into the sensitivity of the design to these changes.

Two module configurations were used: minimodules are 12 x 16 in. (30 x 40 cm) and contain several cells (Figure 2-1), while submodules are 5 x 9 in. (13 x 23 cm) and contain two 4-in. (10-cm) diameter cells (Figure 2-2). Use of the simple two-cell submodules allows comprehensive statistical examination of the behavior of encapsulants, sealants, interconnects, terminations, etc., in a relatively inexpensive manner. In contrast, interactions between nonadjacent cells, effects of unmatched or anisotropic thermal expansion, edge phenomena, etc. may require the larger and more expensive minimodules. Such problems as module stability when subjected to wind loading or out-of-plane torques would require full-scale modules, but are considered design-related rather than materials-related, and so are beyond the scope of this program.

Materials were selected for use in fabricating these test modules on the basis of the following considerations:

(1) suitability of their physical, mechanical, and chemical properties not only in terms of module life but also of module producibility;

(2) availability in sufficient quantity for industrial use at relatively low cost;

(3) lack of available design-related data, including expected materials lifetimes, at the outset of the program;

(4) generality of designs, intended to be representative of concepts which might be used in next-generation modules.

Consequently, several low-cost materials were used to fabricate structural substrates, but only glasses were used as structural superstrates.

Photographs of representative minimodules and large-scale drawings of each type are presented in Appendix B, together with pertinent comments about fabrication methods. Note that Type II minimodules and Type IV submodules were not produced.

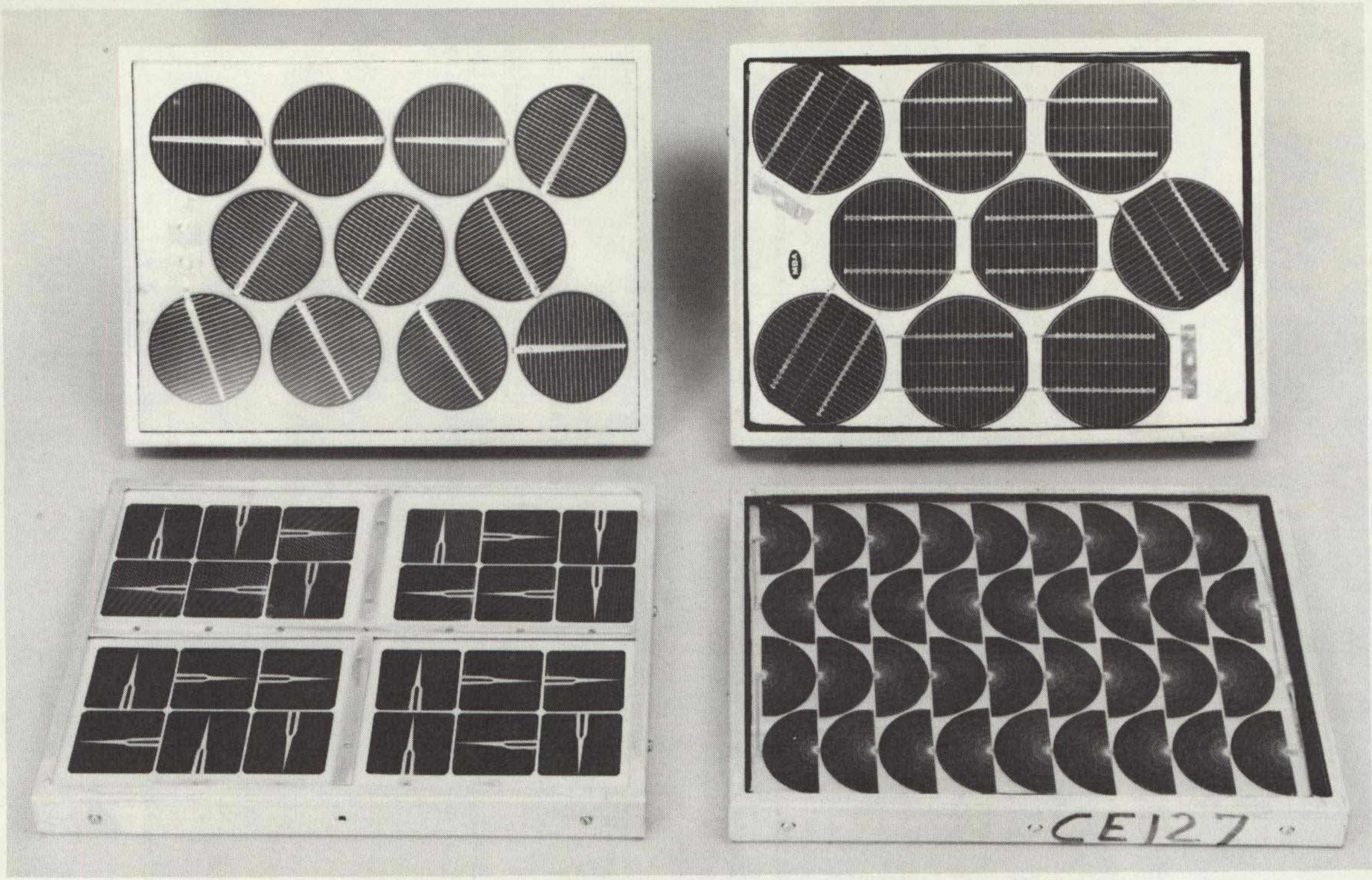

Clockwise from upper left: Springborn, MBAssociates (Type IV), Applied Solar Energy (Type VII), Spire (Type IX).

Figure 2-1. Typical Minimodules

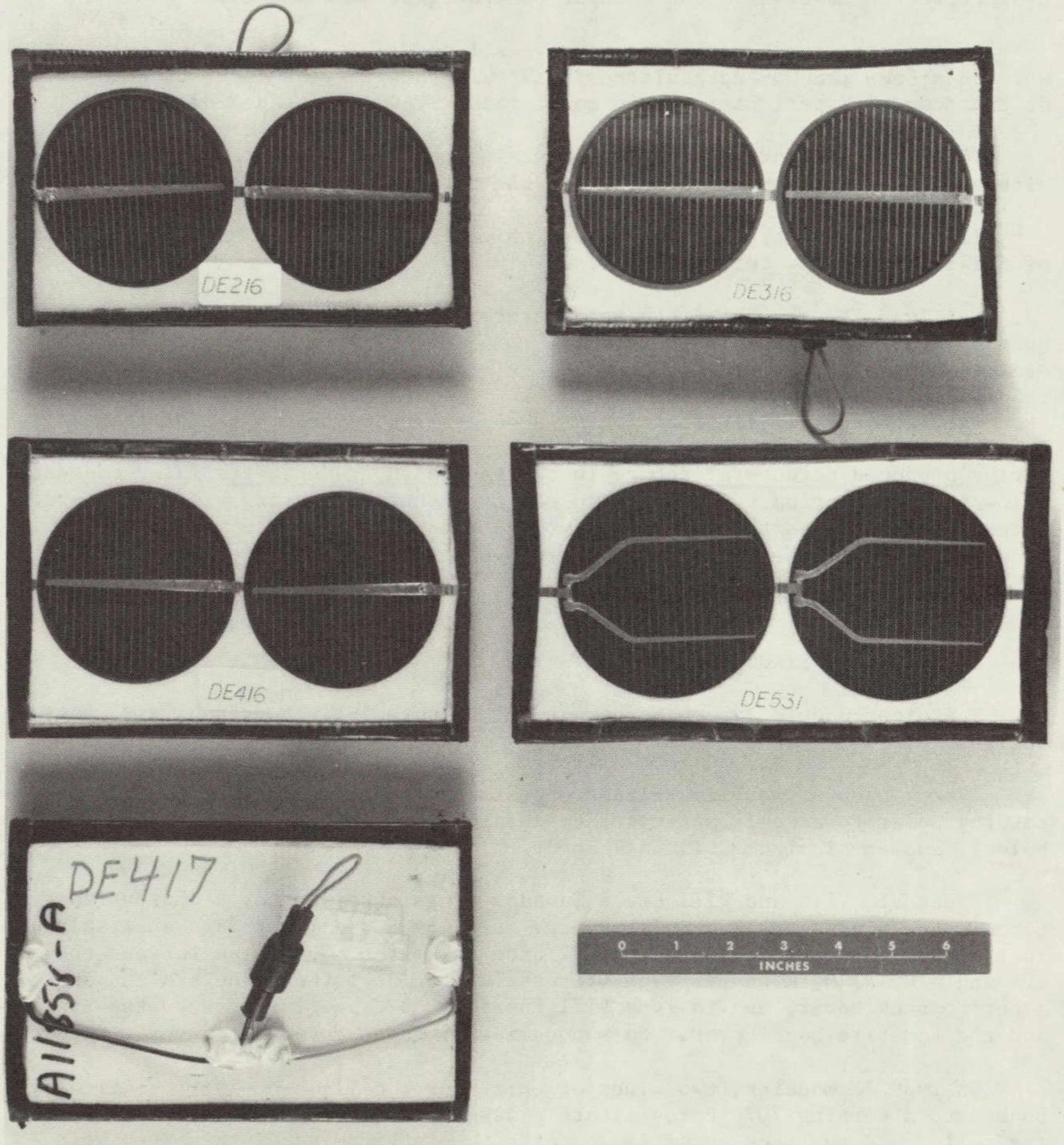

Figure 2-2. Typical Submodules

ORIGINAL PAGE IS
OF POOR QUALITY

B. MODULES WITH STRUCTURAL SUBSTRATES

The first four module types shown in Figure 1-1 are made with structural substrates. The designs are fundamentally the same: the photovoltaic circuit is encapsuated in EVA* (clear above and white below), and sandwiched between a protective top cover film and a layer of Craneglas over the substrate.

The substrate material used for Types I and II is Super Dorlux hardboard which has been vacuum-encapsulated in EVA with a Craneglas layer on each side of the board. Type I has a Korad cover film; Type II uses a Tedlar cover.

The substrate for Type III is galvanized steel, also encapsulated in EVA with a Craneglas layer on each side of the metal; the cover is again Korad.

In these three types, the photovoltaic circuits are the same and make use of Solar Power Corp. cell assemblies.

For Type IV, the substrate is glass-reinforced concrete with an Acmetite moisture barrier on its inner surface. ARCO Solar, Inc. cell strings are used as the photovoltaic circuit.

One particularly important point should be noted here: use of temperatures above 100°C combined with vacuum-bagging to encapsulate the Super Dorlux produced structural damage in the hardboard, reduced its water content below the equilibrium value, and caused it to shrink. During field exposure, water slowly entered the hardboard through the encapsulant films and caused it to expand. These phenomena have led to open-circuit failure of a number of test modules due to cracked cells (cf. Section V).

C. MODULES WITH STRUCTURAL SUPERSTRATES

The eight module Types, V through XII (Figure 1-1), represent five basic designs.

Type V uses a soda-lime glass superstrate, a photovoltaic circuit containing Solar Power cell strings encapsulated in EVA (clear above and white below), and an aluminum-foil back cover.

Types VI, VII, and VIII use a Sunadex glass superstrate, a photovoltaic circuit containing Applied Solar Energy Corp. (ASEC) cell strings encapsulated in EVA, and various backings: Type VI uses a layer of Craneglas between the EVA and a Mylar back cover, Type VII uses Craneglas between the EVA and an Acmetite back cover, and in Type VIII there is no Craneglas between the EVA and the Acmetite back cover. No submodules of these three types were produced.

In Type IX modules, two kinds of Spire Corp. cells are electrostatically bonded to a Corning 7070 borosilicate glass superstrate, EVA seals the back of the cells, and the back cover is Acmetite. No submodules of this type were produced.

*See Appendix A for materials data.

In Type X modules, ASEC cell strings are bonded to a Sunadex glass superstrate by means of an RTV silicone rubber adhesive, then encapsulated in RTV silicone rubber; the back cover film is Acmetite. No submodules of this Type were produced.

Types XI and XII use a soda-lime glass superstrate and ASEC cell strings potted in polyurethane; Type XI has no back cover, while Type XII has an Acmetite film. No submodules of these types were produced.

SECTION III

FACILITIES AND TEST METHODS

A. OVERVIEW

The facilities and test methods used in the laboratory and field evaluation of these minimodules and submodules were developed previously by other FSA Tasks at JPL. Brief descriptions of these facilities and methods are given in this Section; details are provided in the references cited.

Before any testing was carried out, current-voltage (I-V) curves were determined for each minimodule, discrepancies in their construction were charted (cracks, delaminations, etc.), and photographs of both top and bottom were taken. The distribution of modules among the various tests is shown in Table 1-1.

B. LABORATORY TESTS

Representative minimodules of each type were subjected to most of the environmental tests used to qualify full-size commercial modules for the FSA test program at JPL (Reference 1). Those tests not applied were a cyclic mechanical-loading (fatigue) test and a twisted-mounting-surface test, which ensure that electrical opens or shorts to ground do not develop under such conditions. These two tests were determined to be inapplicable because of the minimodule's size and geometry.

1. Environmental-Chamber Testing

Minimodules ready for testing in the Bemco environmental test chamber are shown in Figure 3-1. Parameters for thermal cycling, the first test to which they were subjected, are given in Figure 3-2; those for humidity-freeze cycling, the second test, are shown in Figure 3-3. During each type of test the modules were instrumented and monitored to verify that no open circuits or shorts to ground occurred. Photographs and I-V curves were obtained after completion of each test (I-V curves were made within one hour of removal from the humidity chamber). Details of the test facility can be found in Reference 1.

2. Hail Testing

From the modules which had undergone environmental testing, one of each type was selected for simulated hail testing. For this, artificial ice balls 1 in. (2.5 cm) in diameter were equilibrated at $-10^{o}C$, then shot by an air gun to selected points on the module (Figure 3-4). Each of five points received one impact at terminal velocities of 25, 33, 43, and 52 mi/h (40, 53, 69, and 84 km/h). Testing was terminated if the module was damaged at any velocity lower than 52 mi/h. Details of this test are given in References 1 and 2.

ORIGINAL PAGE IS
OF POOR QUALITY

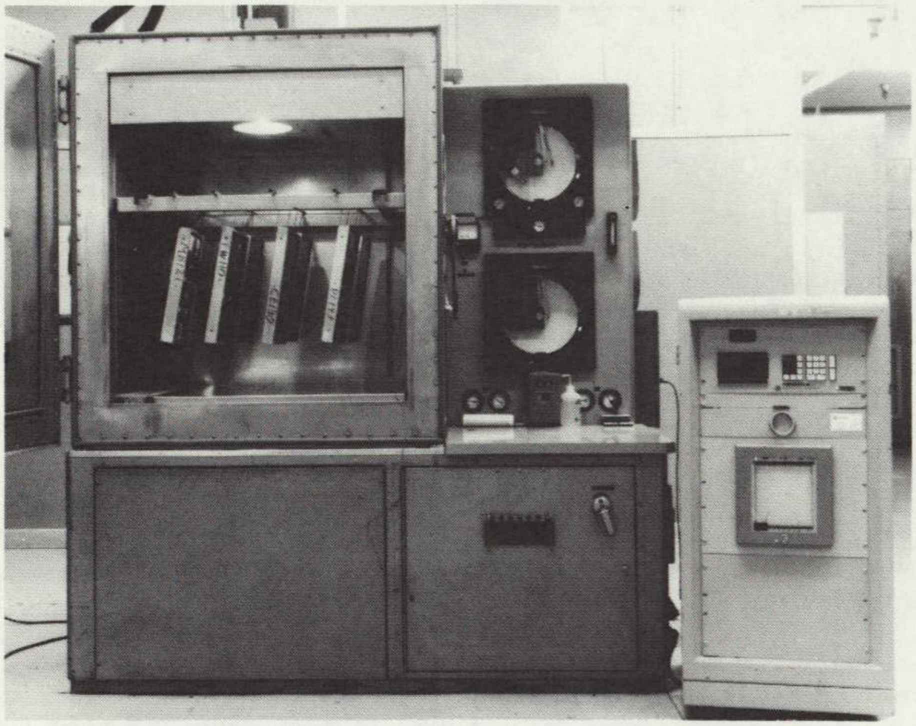

Figure 3-1. Minimodules in Environmental Test Chamber

(SHORTER CYCLE TIME IS ACCEPTABLE IF 100°C/h MAXIMUM RATE OF TEMPERATURE CHANGE IS NOT EXCEEDED. CHAMBER MAY BE OPENED AT 25-CYCLE INTERVALS FOR VISUAL INSPECTION.)

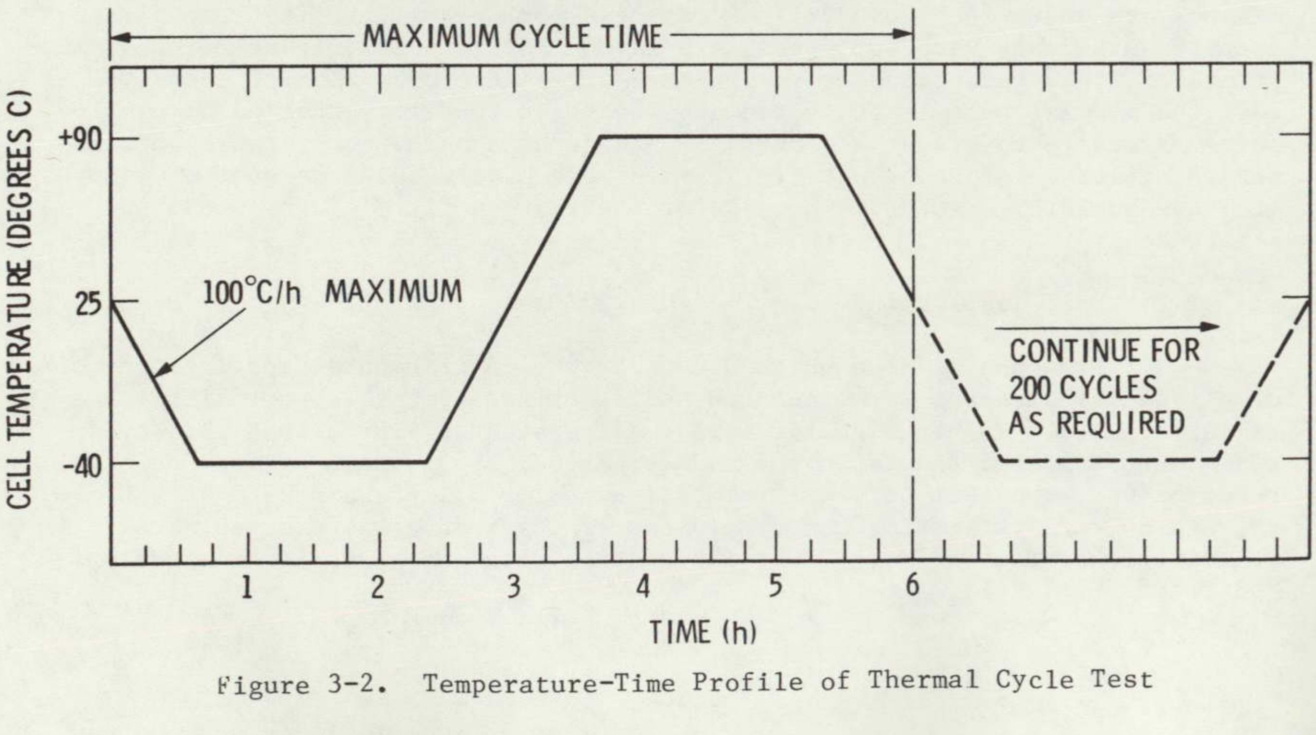

Figure 3-2. Temperature-Time Profile of Thermal Cycle Test

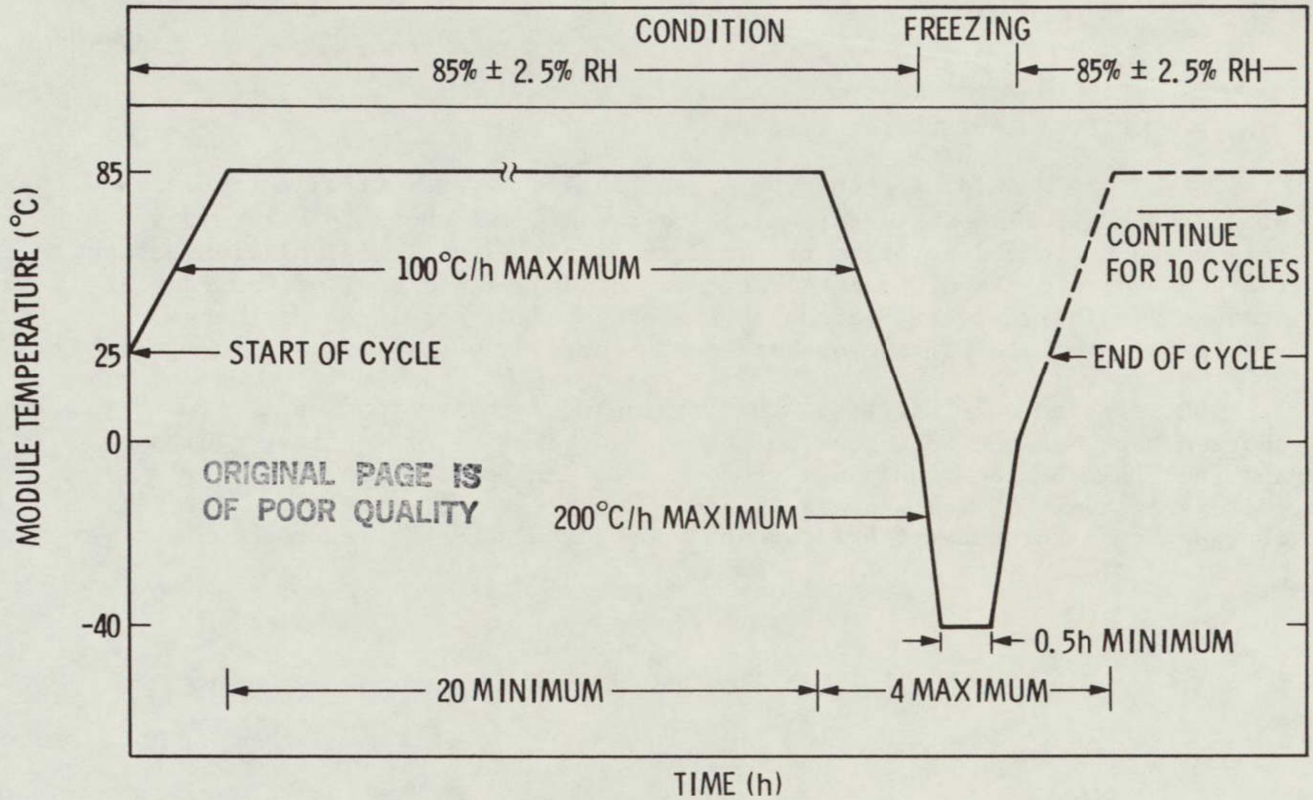

Figure 3-3. Humidity-Temperature-Time Profile of Humidity-Freezing Cycle Test

Figure 3-4. Hail Test System

The minimodule is mounted just above the barrel of the hail gun.

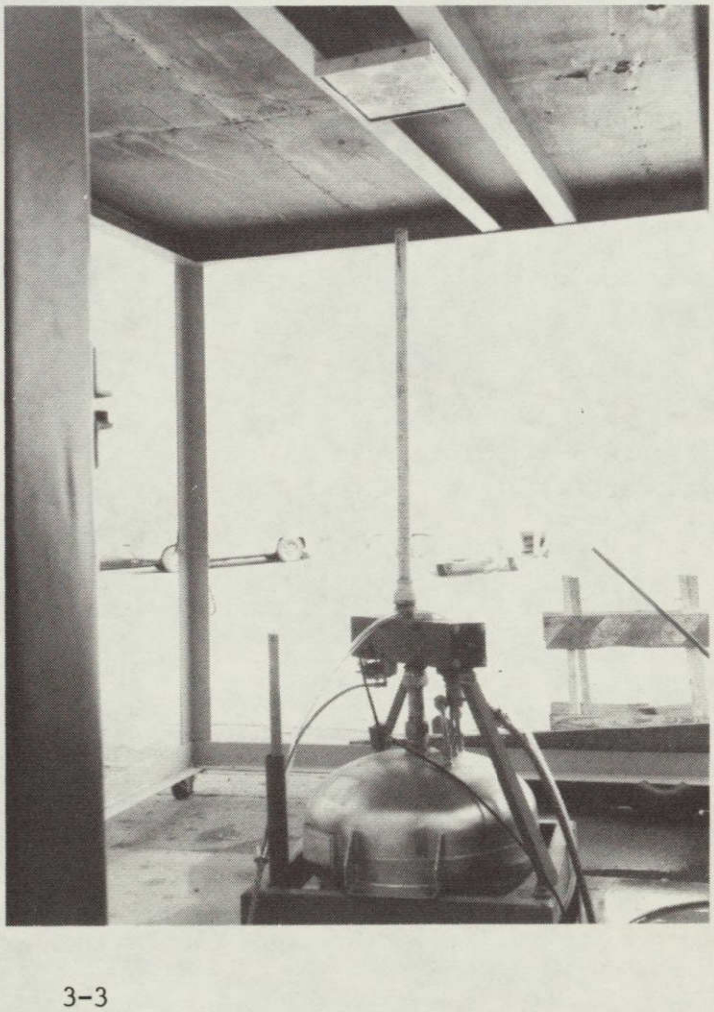

3. Partial-Discharge Testing

One module of each Type except IX and X was tested in the James G. Biddle 40 kV, 3 kVA partial-discharge test equipment shown in Figure 3-5. This was done to characterize the quality of the electrical isolation between the photovoltaic circuit and the frame or ground, since small discharges can produce cumulative deterioration of the encapsulant and large discharges may result in immediate failure or hazard of electric shock.

In carrying out this test, the terminals of the photovoltaic circuit were shorted together and connected to the active terminal of the test equipment, and the frame of the module was connected to equipment ground. A slowly increasing 60-Hz AC voltage was applied, and its value was noted when discharges began to appear ($\approx$0.1 pC) and when the discharges reached 100 pC.

ORIGINAL PAGE IS
OF POOR QUALITY

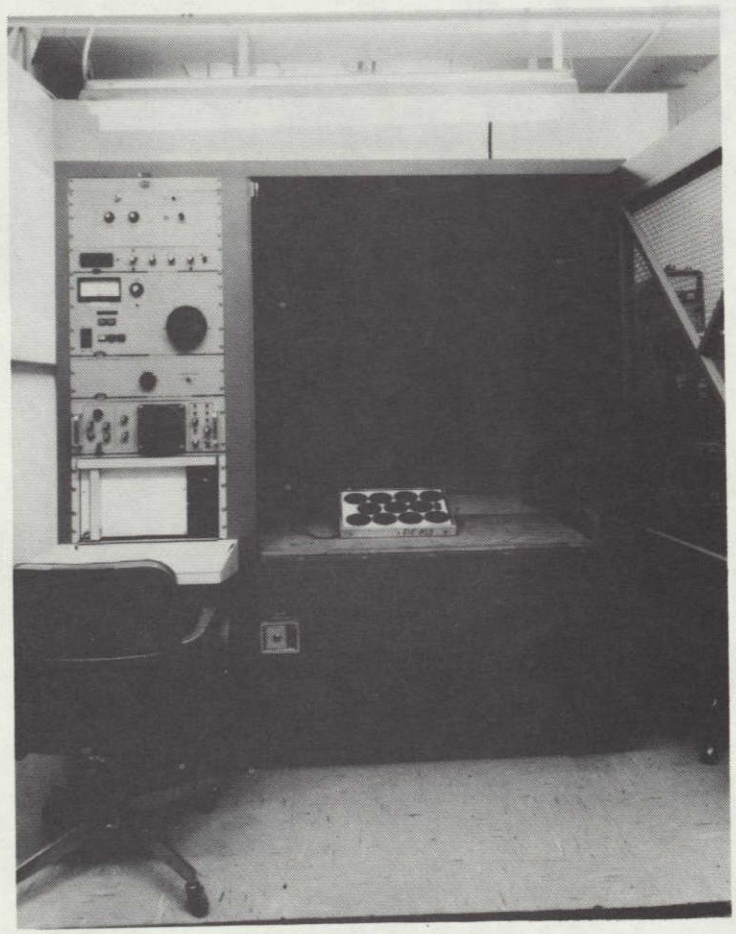

Figure 3-5. Minimodule in Partial Discharge Test Instrument

4. Nominal Operating Cell Temperature (NOCT)

This parameter is the cell temperature when the module, oriented to face the sun at local noon, is operating under open-circuit conditions with a solar irradiance of 80 mW/cm^2 and a 1 m/sec (2 mi/h) wind blowing in 20°C air; it is one of the parameters required for reducing Large Area Pulsed Solar Simulator (LAPSS) I-V curves to standard conditions (cf. Section III.E). The cell temperature is measured at various irradiance levels by means of thermocouples soldered to the back of the cell. Air temperatures measured at the same time are subtracted from the corresponding cell temperatures; this difference is plotted against irradiance to obtain the preliminary NOCT, which is then corrected for air temperature during test and for wind speed. Details are given in Reference 1.

NOCT was determined at JPL for selected single cells of single modules of six types, two with structural substrates and four with structural superstrates; these modules were then available for further testing.

C. ACCELERATED TESTING IN CONCENTRATED SUNLIGHT

Four minimodules and 24 submodules were tested at DSET Laboratories, Inc., Phoenix, Arizona. The minimodules were tested in their SuperMaq machine, a 50-ft (15-m) high sun-tracking Fresnel concentrator whose target area of 18 x 90 in. (0.5 x 2.3 m) is illuminated at 8 suns intensity; air cooling keeps the average cell temperature at not more than 10°C above NOCT.

Eight submodules were tested on an EMMAQUA machine (Equatorial Mount with Mirrors for Acceleration Plus Water Spray). This device, a sun-tracker smaller than the SuperMaq, combines accelerated ultraviolet exposure with periodic water spray (Figures 3-6 and 3-7).

Eight submodules were tested on an EEQUA machine (Equatorial Follow-the-Sun Mount with Water Spray). This also tracks the sun, but does not accelerate the exposure by mirrors.

Finally, eight submodules were tested on racks tipped 34° south, the latitude of the test site.

The minimodules and submodules were inspected visually each week, and periodic I-V curves were obtained by DSET, using solar irradiance. Measurements of solar radiation, ambient temperature, relative humidity, rain, wind, and sky condition were also made during the exposures. Additional information about this test facility can be found in Reference 3.

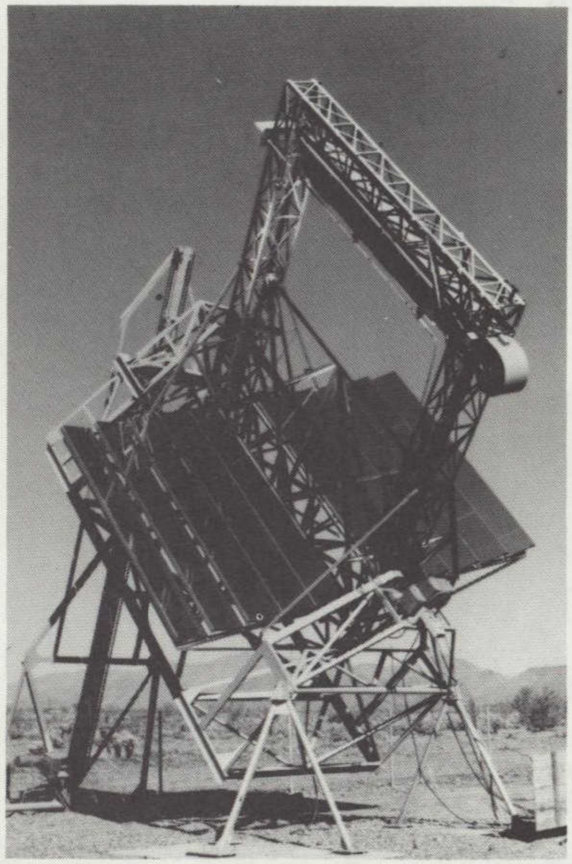

Figure 3-6. DSET EMMAQUA Accelerated-Exposure Test Machine

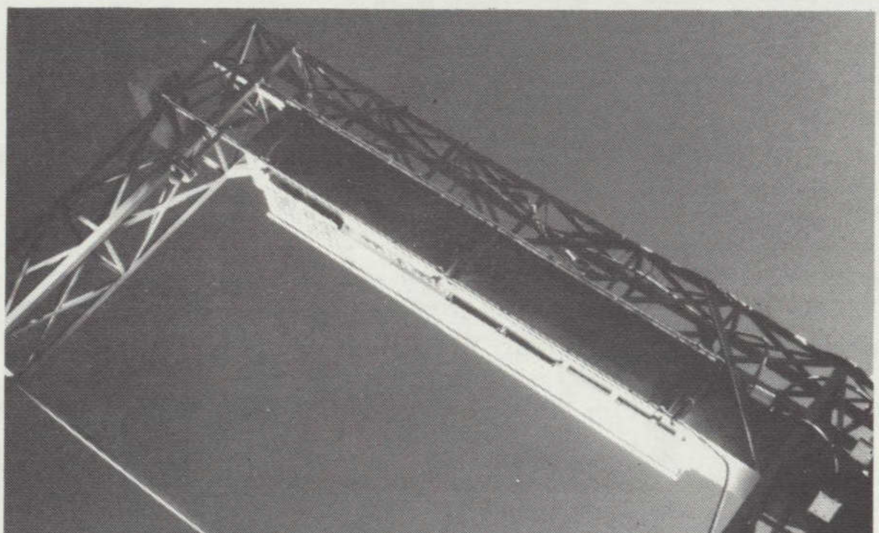

Figure 3-7. Minimodules Mounted at the Target Area of a DSET EMMAQUA Test Machine

D. FIELD EXPOSURE

Three locations in Southern California were selected for field aging of both minimodules and submodules: the JPL site (Figure 3-8) is in a smoggy urban area, Pasadena, at the foot of the San Gabriel Mountains; JPL's Goldstone Tracking Station (Figure 3-9) is in the center of the Mojave Desert; the Pt. Vicente test site (Figure 3-10) was just outside the U.S. Coast Guard Station on the Palos Verdes peninsula of Los Angeles, a corrosive coastal location. This latter site was deactivated for nine months because of module thefts. Although a chain-link fence was installed around the test facility during this time, it did not deter the thieves, and this site was finally abandoned in June 1982.

All modules were mounted on racks facing south at an angle of approximately 34° from the horizontal.

The terminals of the submodules were shorted together, but the minimodules were loaded with one 10-Ω, 12-W resistor in parallel with a type 313 miniature lamp, which has a resistance in excess of 150 Ω when hot (Figure 3-11). This load is near that producing maximum power output from most of these test modules.

Modules were removed for periodic visual inspection and electrical performance testing in the JPL LAPSS Facility (Section III. E) at the intervals shown in Table 3-1. These measurements were made first while the modules were as-weathered (dirty) and then after they had been washed with detergent--8 oz Franklin Formula 707 heavy-duty water-base degreaser per 1 gal of water (60 mℓ/ℓ)--using a sponge, rinsed with tap water, and dried with a chamois. (The initial cleaning procedure, which used a squeegee, may have damaged several modules--cf. modules DE105, Table C-2, and DE107, Table C-3.)

Table 3-1. Intervals Between Examinations of Field-Exposure Modules

Site	Module Size	Intervals, months	Last Exam
JPL	mini	1-1-1-3-4-9-6	8/20/82
	sub	7-5	7/20/81
Goldstone	mini	1-2-1-4-7-1-5	9/1/82
	sub	1-1-1	6/23/81
Pt. Vincente	mini	1.5-1.5-1-*-1-3-2	6/17/82 (discontinued)
	sub	1	3/14/81 (discontinued)

*269 days of storage in the dark.

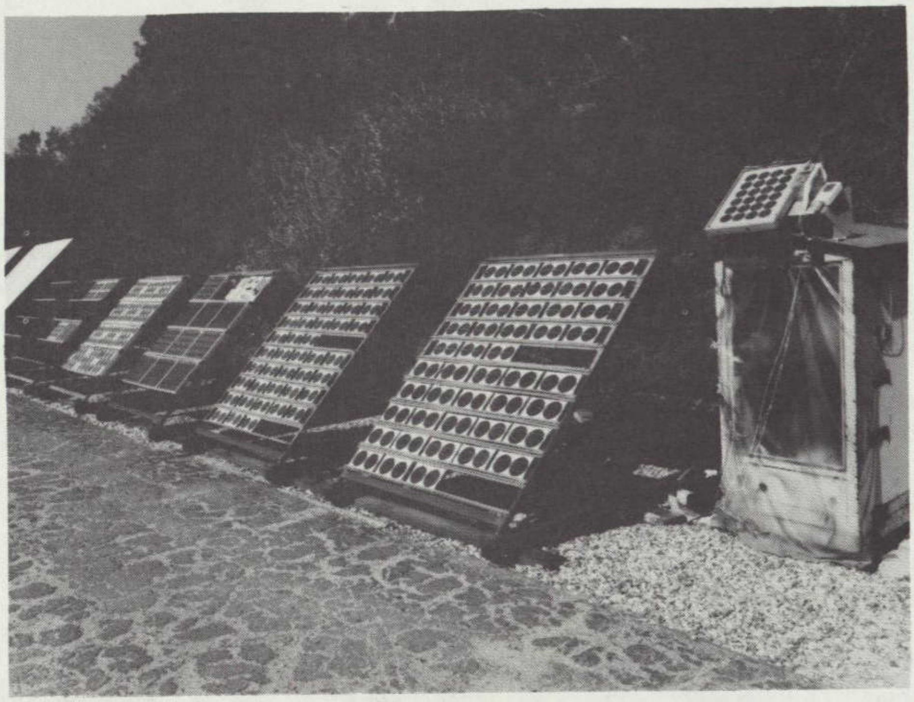

Figure 3-8. JPL Field Exposure Site

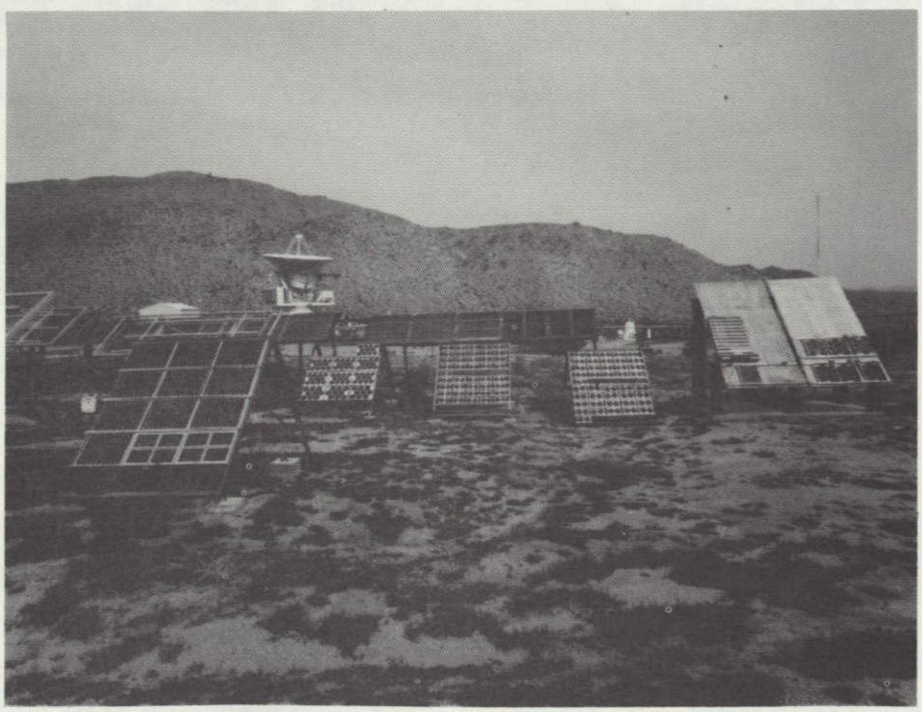

Figure 3-9. Goldstone Field Exposure Site

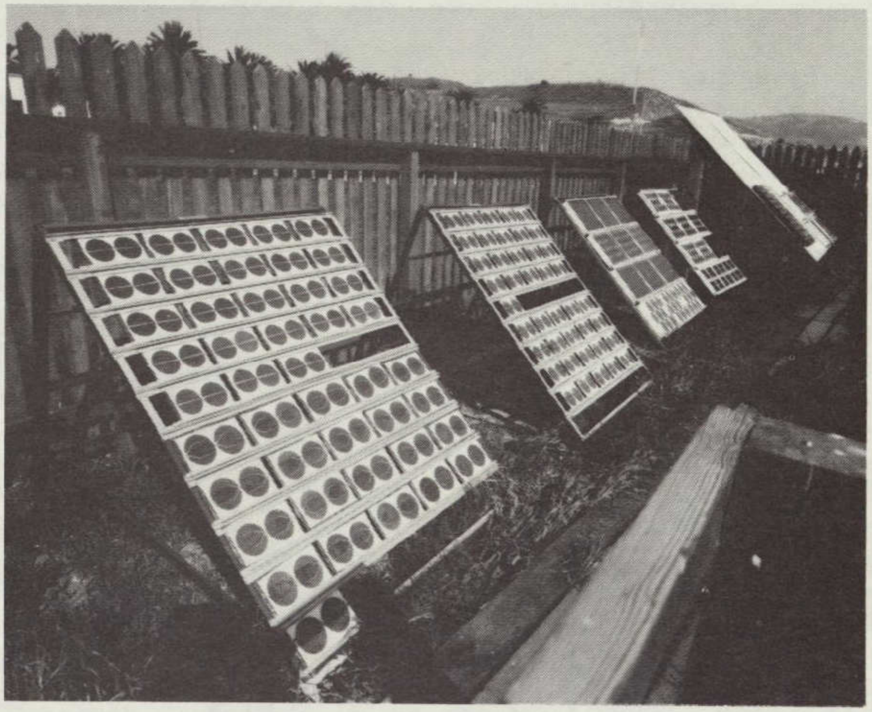

Figure 3-10. Pt. Vicente Field Exposure Site

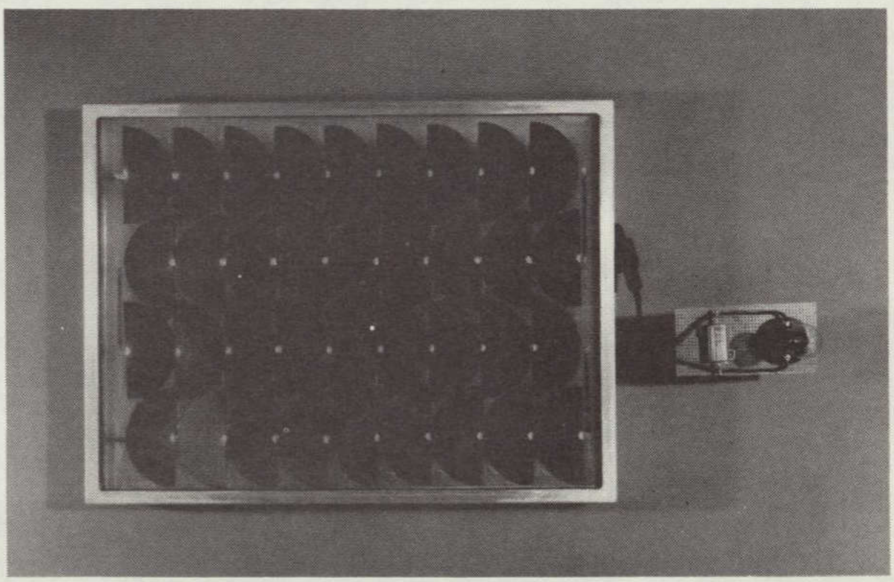

Figure 3-11. Electrical Load on an Applied Solar Energy Minimodule

E. ELECTRICAL PERFORMANCE TESTING

Performance degradation was monitored by means of I-V curves obtained in one of the two Large-Area Pulsed Solar Simulator (LAPSS) devices at JPL before and after each environmental-chamber test, and also before and at selected intervals during the real-time outdoor exposure. This equipment, manufactured by Spectrolab, Inc., consists of two major subsystems: the pulsed light source and the data-acquisition and processing system (Figures 3-12 and 3-13). The light source contains two xenon flash lamps powered by the discharge of a 2000-mF, 5000-V capacitor. During the 3-ms light pulse that results, a high-speed electronic load connected to the module under test is swept from short circuit to open circuit. At 20-μs intervals the voltage and current output by the module are sampled, as is the current from a reference cell. These data are stored and processed with due attention to spectral characteristics of the xenon flash, to the NOCT of the module, etc., to produce the I-V curve of the module and to determine its maximum power output, P_{max}. Changes in maximum power of 5% or more are considered significant. Variations of about this magnitude can be expected from the inherent precision of each LAPSS itself, from slight differences between the two LAPSS machines, and from variations in technique from one operator to another. An apparent "recovery" phenomenon visible in the minimodules exposed at Pt. Vicente (Table C-3) is due to these causes; storage in the dark for 269 days seems to increase the maximum power output by several percent for some months. However, the minimodules from JPL and Goldstone also show an increase in output at the same time, the fall of 1981. Changes in instruments and in operators led to an offset in the data.

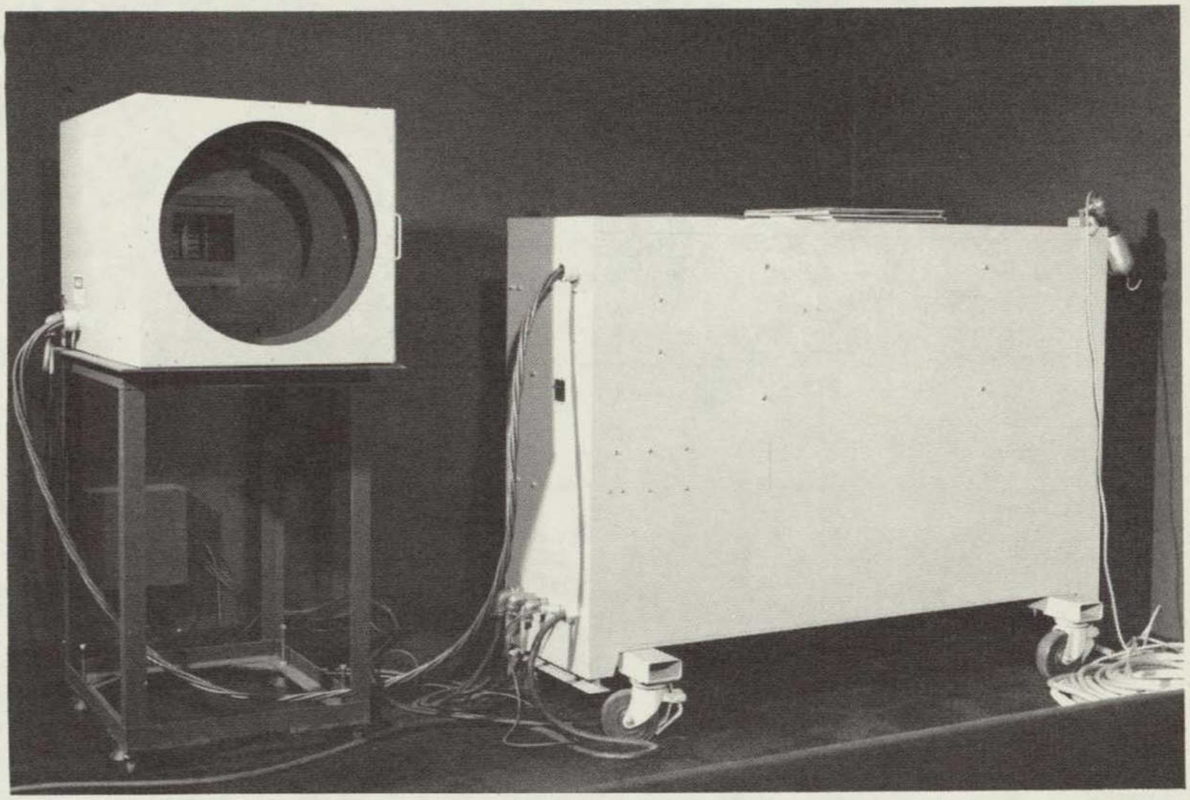

Figure 3-12. LAPSS Lamp and Power Supply

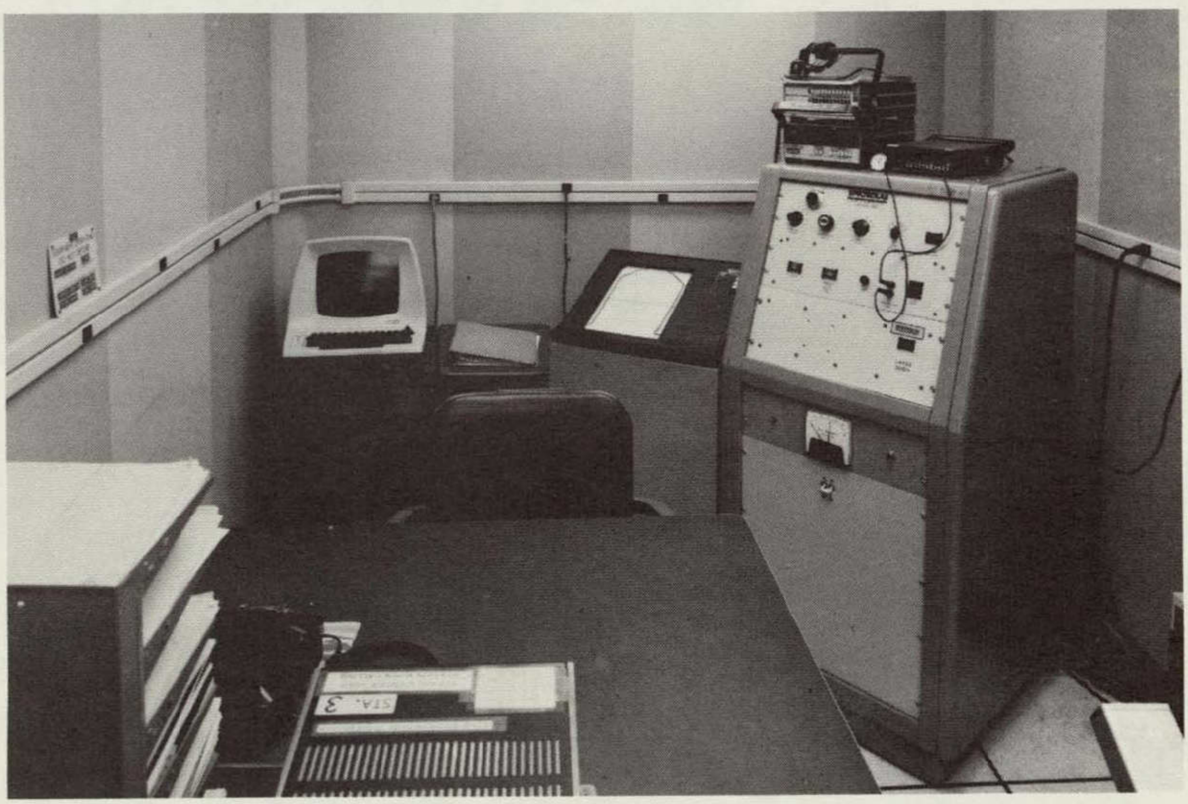

Figure 3-13. LAPSS Data Acquisition and Processing System (with the electronic load at the right)

SECTION IV

SUMMARY OF TEST RESULTS

A. LABORATORY TESTS

1. Environmental-Chamber Testing

Table 4-1 provides a concise overview of the environmental results: maximum power output (P_{max}) after each test is compared with the value before test; there are also results of visual inspection after testing. Since only a change of 5% or more in power output is considered significant, averages have been rounded off to the nearest 5%. In the case of the Type I modules, one showed major power loss after temperature cycling; the average power loss was calculated for the two relatively unaffected modules, and the outlying value is given in parentheses. Similarly, after humidity-freeze testing, a second module showed major degradation; the average power loss is now for the two degraded modules and the value for the essentially undamaged module is given in parentheses.

Three designs degraded significantly during temperature cycling: Types I, III, and V; further degradation occurred during humidity-freeze testing of Types I, IV, and IX. These include all the designs with structural substrates --in particular two of the three modules incorporating Super Dorlux (Type I) showed dramatic power losses. This is related to the module manufacturing process, as discussed in Section V. The modules incorporating galvanized steel (Type III) showed only borderline changes after temperature cycling and little change after humidity-freeze cycling. The encapsulant was wrinkled after each test, however, and probably cracked one or more cells as it deformed. Those with glass-reinforced concrete substrate (Type IV) withstood temperature cycling rather well but degraded during humidity-freeze cycling, when distortion of the encapsulant again led to cell cracking.

Of the other designs with evidence of degradation, Type V (glass superstrate, EVA encapsulant, and aluminum backing) showed borderline power loss after temperature cycling and little change during humidity-freeze cycling; once more, the encapsulant wrinkled during test. Type IX (cells electrostatically bonded to Corning 7070 borosilicate glass, EVA encapsulant, Acmetite backing) showed no loss after temperature cycling, yet one of the two modules failed completely after humidity-freeze cycling while the other showed no change. In both cases the glass superstrate cracked during test, which also cracked one or more cells; in one case this apparently opened the photovoltaic circuit, while in the other it did not.

Table 4-1. Summary of Minimodule Temperature and Humidity-Freeze Testing

	P_{max}, watts (% change)			Comments	
Serial Number	Original	After Temp. Test	After Humidity-Freeze Test	After Temp. Test	After Humidity-Freeze Test
TYPE I					
DE111	6.24	6.09 (-2.4%)	5.88 (-5.8%)	Cracked cell, film wrinkled, edge discoloration	Encapsulant discoloration, interconnects distorted
DE112	6.81	2.54 (-62.7%)	1.83 (-73.1%)	Cracked cell	Interconnect distorted, splits in surface film
DE113	6.29	5.95 (-5.4%)	0.12 (-98.1%)	Delamination	Interconnect distorted, splits in surface film
	average:	-5% (-60%)	-85% (-6%)		
TYPE III					
DE141	6.71	6.48 (-3.4%)	6.35 (-5.4%)	Delamination, wrinkled, film encapsulant discoloration at edges	Edge sealant flow, splits in surface film
DE142	6.50	6.09 (-7.6%)	5.98 (-8.0%)	Wrinkled film	Edge sealant flow, splits in surface film
DE143	6.28	6.12 (-2.5%)	6.05 (-3.7%)	Wrinkled film	Edge sealant flow, splits in surface film
	average:	-5%	-5%		
TYPE IV					
MB121	7.87	7.40 (+0.4%)	7.14 (-9.3%)	Sealant extrusion, delamination	Splits in cover, hardware corrosion
MB122	7.94	7.81 (-1.6%)	6.46 (-18.6%)	Cracked cell, delamination, splits in cover	Splits in cover, hardware corrosion
MB123	8.85	9.06 (+2.3%)	8.33 (-5.9%)	Delamination	Splits in cover, hardware corrosion
	average:	0	-10%		

Table 4-1. Summary of Minimodule Temperature and Humidity-Freeze Testing (cont'd)

Serial Number	P_{max}, watts (% change)			Comments	
	Original	After Temp. Test	After Humidity-Freeze Test	After Temp. Test	After Humidity-Freeze Test
TYPE V					
DE127	6.05	5.82 (-3.8%)	5.59 (-7.6%)	Al foil wrinkled	Encapsulant discolored at edges, interconnect distorted
DE128	6.24	5.96 (-4.5%)	5.96 (-4.5%)	Al foil wrinkled, encapsulant discoloration	Edge sealant flow
DE129	6.34	6.05 (-4.6%)	5.98 (-5.7%)	Al foil wrinkled, cracked cell	Edge sealant flow, encapsulant discoloration at edges
	average:	-5%	-5%		
TYPE VI					
CE112	11.24	11.08 (-1.4%)	11.19 (-0.4%)	No Change	Sealant tacky
CE114	10.51	10.28 (-2.2%)	10.23 (-2.7%)	Gas pockets moved to back of cells	Sealant tacky, delamination
CE115	10.68	10.45 (-2.2%)	10.50 (-1.7%)	Gas pockets moved to back of cells	Sealant tacky, delamination
	average:	0	0		
TYPE VII					
CE128	10.83	10.65 (-1.7%)	10.69 (-1.3%)	Gas pockets moved under cells, Al foil wrinkled	Sealant tacky, encapsulant discoloration
CE129	10.88	10.65 (-2.1%)	10.65 (-2.1%)	Gas pockets moved under cells, Al foil wrinkled	Gas pockets
CE130	10.69	10.50 (-1.8%)	10.58 (-1.0%)	Gas pockets moved under cells, Al foil wrinkled	Sealant tacky, encapsulant discoloration at edges
	average:	0	0		

Table 4-1. Summary of Minimodule Temperature and Humidity-Freeze Testing (cont'd)

Serial Number	P_{max}, watts (% change)			Comments	
	Original	After Temp. Test	After Humidity-Freeze Test	After Temp. Test	After Humidity-Freeze Test
TYPE VIII					
CE143	10.61	10.67 (+0.6%)	10.78 (+1.6%)	Foil backing wrinkled	Frame hardware corrosion
CE144	10.67	10.77 (+0.9%)	10.72 (+0.5%)	Foil backing wrinkled	Frame hardware corrosion
CE145	11.02	11.49 (+4.5%)	11.18 (+1.5%)	Foil backing wrinkled	Frame hardware corrosion
	average:	0	0		
TYPE IX					
SE104	8.68	8.75 (+0.8%)	8.70 (+0.2%)	Delamination	Glass cracked, cell cracked
SE122	5.49	----	Open	Delamination	Glass cracked, delamination, hardware corrosion
	average:	0	0,-100%		
TYPE X					
GE105	10.45	10.60 (+1.4%)	10.63 (+1.7%)	Sealant extrusion, delamination	Frame hardware corrosion
	average:	0	0		
TYPE XI					
PW109	6.01	---	5.55 (-7.7%)	No inspection, see "After Humidity Test"	Sealant extrusion, hardware corrosion, discoloration, gas pockets
PW110	5.36	---	5.62 (+4.9%)	No inspection, see "After Humidity Test"	Hardware corrosion, discoloration, gas pockets
PW111	4.39	4.63 (+5.5%)	4.64 (+5.7%)	Discoloration	No inspection
	average:	+5%	0		

ORIGINAL PAGE IS OF POOR QUALITY

Table 4-1. Summary of Minimodule Temperature and Humidity-Freeze Testing (cont'd)

Serial Number	P_{max}, watts (% change)			Comments	
	Original	After Temp. Test	After Humidity-Freeze Test	After Temp. Test	After Humidity-Freeze Test
TYPE XII					
PW124	7.33	7.24 (-1.5%)	7.15 (-2.5%)	No inspection, see "After Humidity Test"	Wrinkled Al, delamination, hardware corrosion
PW125	6.15	6.12 (-0.5%)	6.02 (-2.1%)	No inspection, see "After Humidity Test"	Wrinkled Al, delamination
PW126	6.32	6.81 (+7.8%)	6.88 (+8.9%)	No inspection,see "After Humidity Test"	Wrinkled Al, delamination, hardware corrosion
	average:	0	0		

2. Hail Testing

Only two of the modules tested exhibited any signs of damage (Table 4-2). The Type VII module (CE130) cracked during the third impact at 52 mi/h (84 km/h) (Figure 4-1a). The position struck was near the edge of the panel and failure may have been due to an edge flaw in the glass superstrate. The Type IX module (SE104) cracked at each of the first four impacts at 25 mi/h (40 km/h), so testing was stopped (Figure 4-1b). It should be noted, however, that none of these failures were related to the crack which formed during humidity-freeze testing.

Table 4-2. Summary of Minimodule Hail Testing

Type	Serial Number	Result
Substrate		
I	DE113	Passed
III	DE143	Passed
IV	MB121	Passed
Superstrate		
V	DE127	Passed
VI	CE114	Passed
VII	CE130	Cracked at edge only, third impact at 52 mi/h (84 km/h)
VIII	CE143	Passed
IX	SE104	Failed: 4 cracks at 25 mi/h (40 km/h)
X	GE105	Passed
XI	PW110	Passed
XII	PW126	Passed

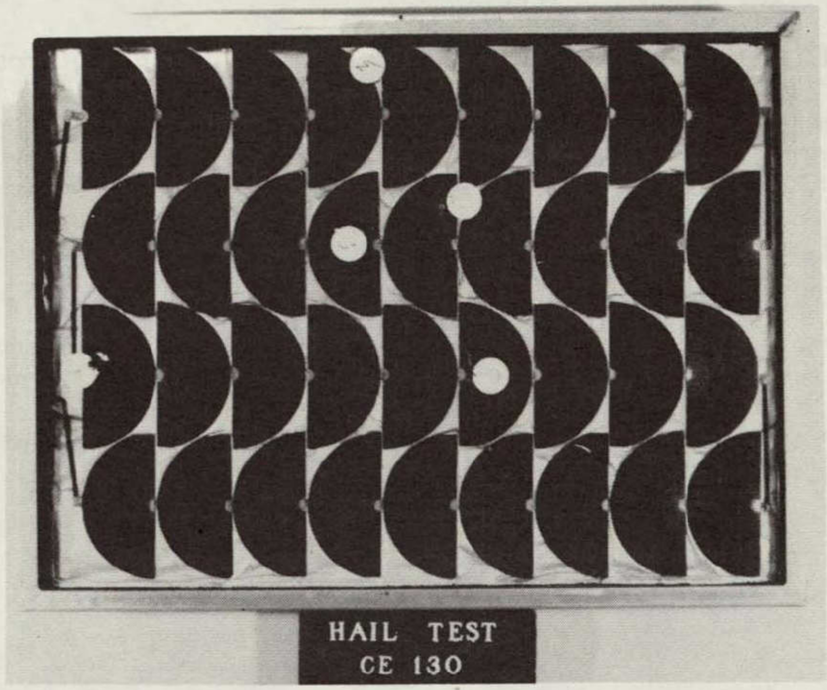

a. Type VII Minimodule

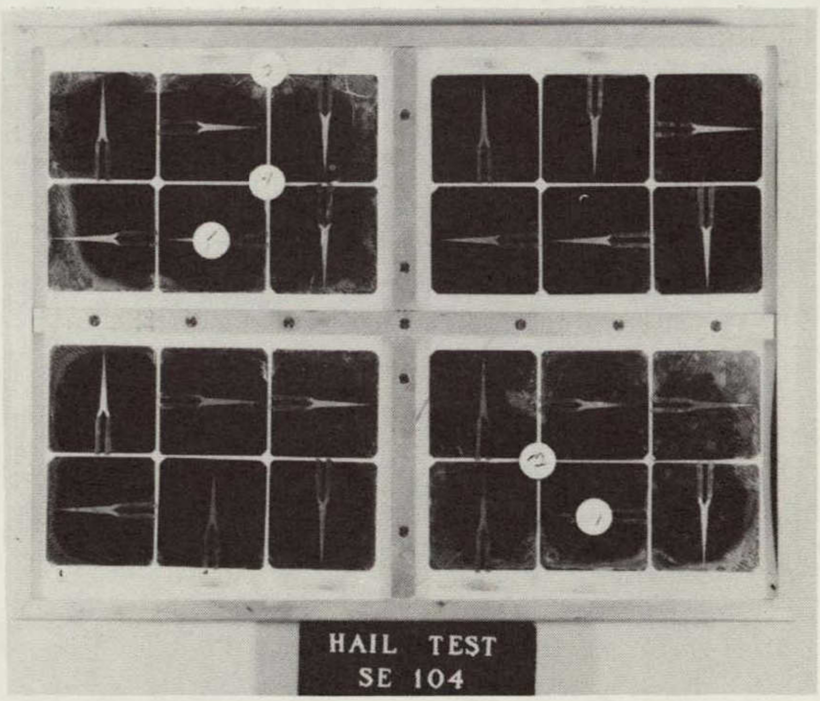

b. Type IX Minimodule

Figure 4-1. Minimodules Which Failed Hail Test (labels indicate impact points)

3. Partial Discharge Testing

All module designs except those incorporating electrostatically bonded cells (Type IX) or RTV encapsulant (Type X) were evaluated in the JPL partial-discharge test facility; results are given in Table 4-3. In reviewing these data, it is important to remember that at an inception level of approximately 20 pC, the higher the values of both rms and peak test voltage, the better the module; the same is true at the 100-pC level. An accepted rule of thumb is that the inception voltage should be three to five times the operating voltage.

The comments as to type of partial discharge or other observations are important because leakage paths or shorts typically indicate a design or manufacturing flaw. A notation of "charging effect" indicates a floating ground. This effect is seen in two of the three superstrate designs which incorporate Acmetite film as the back cover (Types VIII and XII).

Table 4-3. Summary of Minimodule Partial Discharge Testing

Type	Serial Number	Partial Discharge at Inception: Test Voltage, kV RMS	Peak	Charge, pC	Type of Partial Discharge	Partial Discharge at ≈100 pC Level: Test Voltage, kV RMS	Peak	Charge pC	Type of Partial Discharge	Notes	Performance
I	DE110	4.6	6.44	25	Void	4.9	6.86	150	Voids		Very good
III	DE140	0.09	0.126	N.A.	19.5 kΩ leakage path	-	-	-	-		Failed
IV	MB119	1.0	1.4	20	Voids	1.35	1.89	103	Voids		OK
V	DE116	250Ω short between frame and cell									Failed
VI	CE108	1.3	1.82	40	Void	1.6	2.24	225	Voids		OK
VII	CE127	1.1	1.54	60	Voids	1.25	1.75	160	Voids		OK
VIII	CE131	1.0	1.4	30	Voids	1.1	1.54	101	Voids		
	CE131	Rerun after trimming thermocouple leads				1.3	1.82	200	Flashover, void	Charging effect	OK
XI	PW107	1.8	2.52	25	Point to plane on frame	2.4	3.36	102	Point to plane on frame		OK
XII	PW122	-	-	-	-	0.5	0.7	230	Surface condition	Flashover at thermo-couple, charging effect	Failed

Notes: All tests performed at room temperature. Types IX and X were not tested.

4. Nominal Operating Cell Temperature (NOCT)

NOCT values ranged from 40° to 46°C (Table 4-4), significantly below those reported for commercial modules in Block III, 46° to 61°C (Reference 4), and Block IV, 46° to 58°C (Reference 5).

Table 4-4. Minimodule Nominal Operating Cell Temperature (NOCT)

Type	Serial Number	NOCT, °C
I	DE114	45.7
III	DE145	39.8
V	DE116	45.5
VI	CE109	42.2
VII	CE116	42.9
VIII	CE131	44.0

B. ACCELERATED TESTING IN CONCENTRATED SUNLIGHT

Although analysis of this portion of the program has not been completed, several results can be reported now.

Three of the four minimodules exposed on the SuperMaq failed: DE114 (Type I), CE116 (Type VII), and SE103 (Type IX). I-V curves obtained by DSET shortly after failure are shown in Figure 4-2; unfortunately, because of operational problems, only the shapes of the curves are meaningful, while actual numerical values may not be directly compatable to those obtained with a JPL LAPSS. Information from the final weekly inspection reports for these modules is presented in Table 4-5.

Submodules tested on the EMMAQUA are listed in Table 4-6, together with information from the final inspection report. None of these modules showed gross failure through their I-V curves, but modules DE502 and DE503 (Type II) did show considerable structural damage. Interestingly, the other modules containing Super Dorlux, DE405 and DE410, were not quite as strongly affected.

One of the eight submodules exposed on the EEKQUA failed, DE440 (Type I), as did one of the eight submodules exposed on the 34°S racks, DE242 (Type V). I-V curves obtained by DSET after exposure of these modules was completed are shown in Figure 4-3.

More complete physical examinations, LAPSS I-V curves, and failure analysis of the nonfunctional modules will be required before more can be said about these tests.

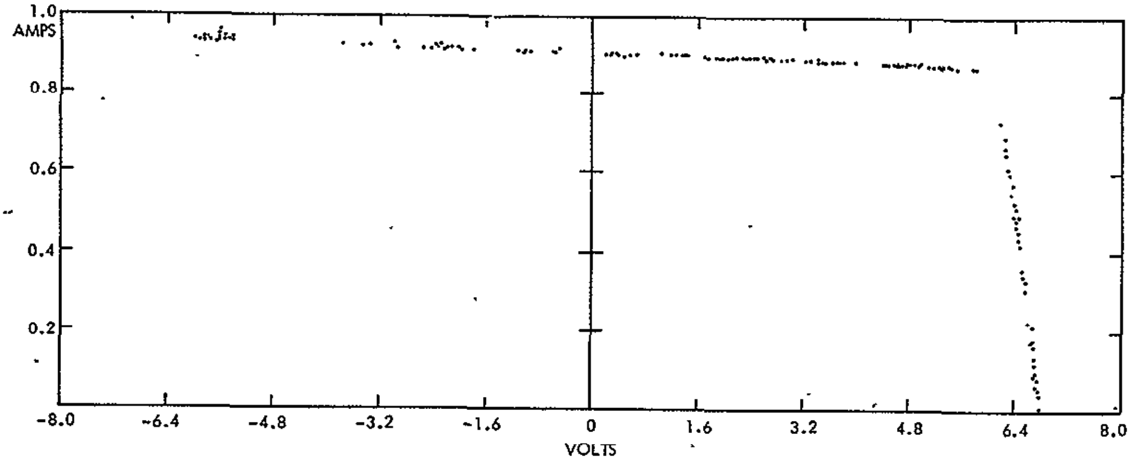

NORMALIZED DATA

Parameter	This Curve	Initial Curve*
V_{OC}	6.79 V	6.495 V
I_{SC}	0.91 A	1.448 A
$V_{P_{max}}$	5.96 V	5.070 V
$I_{P_{max}}$	0.85 A	1.373 A
P_{max}	5.07 W	6.96 W

Module DE114 (Type I) after failure in Super Maq Test

693,970 langleys (20,230 langleys of UV)

*Initial curve from JPL LAPSS measurements.

a. DE114 (Type I)

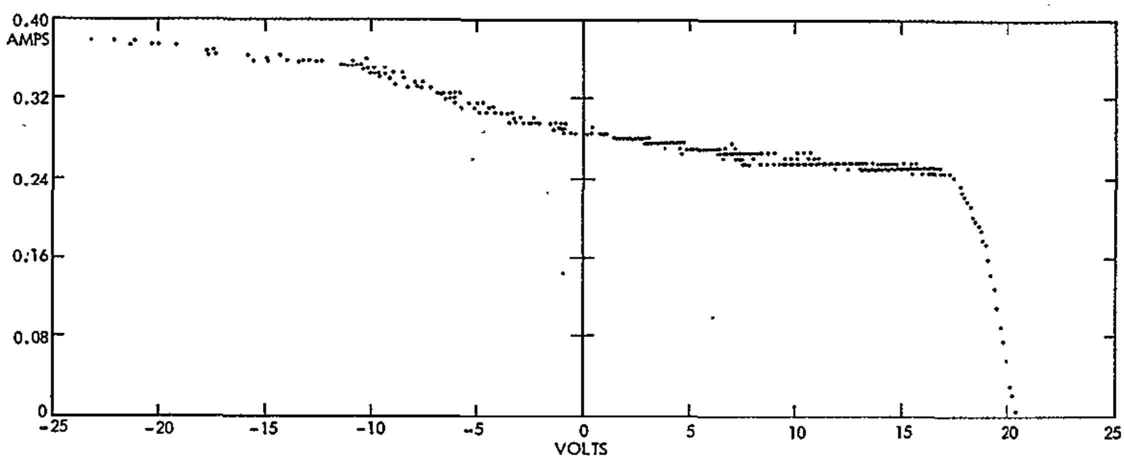

NORMALIZED DATA

Parameter	This Curve	Initial Curve*
V_{OC}	20.34 V	21.123 V
I_{SC}	0.28 A	0.688 A
$V_{P_{max}}$	17.6 V	17.658 V
$I_{P_{max}}$	0.24 A	0.626 A
P_{max}	4.24 W	11.05 W

Module CE116 (Type VII) after failure in Super Maq Test

345,580 langleys (8,096 langleys of UV)

*Initial curve from JPL LAPSS measurements

b. CE116 (Type VII)

Figure 4-2. I-V Curves of Modules Which Failed DSET SuperMaq Accelerated Exposure Test

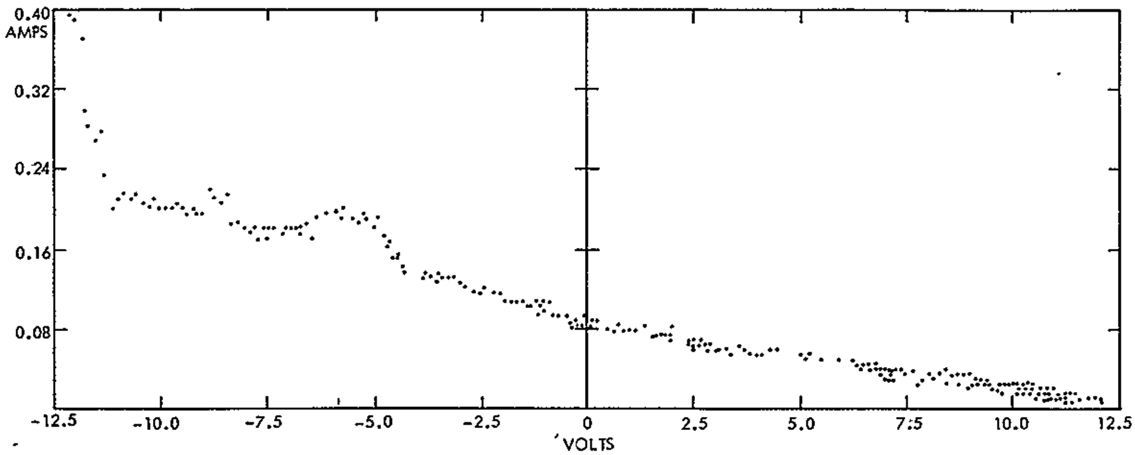

NORMALIZED DATA

Parameter	This Curve	Initial Curve*
V_{OC}	-12.5 V	13.509 V
I_{SC}	~0.09 A	1.029 A
$V_{P_{max}}$	8.4 V	10.701 V
$I_{P_{max}}$	0.04 A	0.938 A
P_{max}	0.3 W	10.04 W

Module SE103 (Type IX) after failure in Super Maq Test

255,550 langleys (8,737 langleys of UV)

Note. Glass cover cracked as described in inspection.

*Initial curve from JPL LAPSS measurements.

c. SE103 (Type IX)

Figure 4-2. I-V Curves of Modules Which Failed DSET SuperMaq Accelerated Exposure Test (cont'd)

Table 4-5. Final *in situ* Inspection Report: Minimodules Tested on DSET SuperMaq

Module Serial Number	General Appearance	Color Change	Carbonization	Cracking	Delamination	Cell Haziness	Encapsulant Haziness	Cumulative Remarks	Total Exposure
DE114	7	7	9	6	8	9	8	Edge discoloration of encapsulant. Discoloration of metallization.	872,770 langleys (4.5 years real-time)
DE145	7	8	9	6	8	9	9	Edge discoloration of encapsulant. Discoloration of metallization.	
SE103	7	7	10	6	8	10	10	Glass cover of module surface cracked (one crack). Discoloration of metallization and part of cell surface at area of crack in glass cover. Three small additional cracks in area of large crack.	527,190 langleys (2.5 years real-time)
CE116	7	8	8	6	10	10	10	Glass cover cracked. Voids. Slight discoloration of metallization.	320,260 langleys (1.75 years real-time)

Key:
10 as received
9 excellent
8 good
7 good to fair
6 fair
5 fair to poor
4 poor
3 poor to very poor
2 very poor
1 extremely poor

Note: 1 langley = 1 calorie/cm^2 = 4.19×10^4 J/m^2

Table 4-6. Final *in situ* Inspection Report: Submodules Tested on DSET EMMAQUA

Module Serial Number	General Appearance	Color Change	Carbonization	Cracking	Delamination	Cell Haziness	Encapsulant Haziness	Discoloration	Cumulative Remarks
DE205	6	6	10	9	10	10	10	6	Small void at cell. Crack upper right corner. Slight yellowing of encapsulant.
DE213	6	6	10	6	8	9	10	6	One crack approximately 6 in. (15 cm) long.
DE305	7	8	10	7	7	9	9	8	
DE312	7	8	10	7	8	8	8	8	Slight wrinkling of substrate. White spot on cell.
DE405	5	7	10	5	7	8	8	7	Slight wrinkling of substrate.
DE410	5	7	10	5	7	8	8	7	Voids.
DE502	4	7	10	3	3	7	7	7	Slight wrinkling of substrate. Voids.
DE503	4	7	10	3	4	7	8	7	Slight wrinkling of substrate. Small void at cell.

Key:

10	as received	5	fair to poor
9	excellent	4	poor
8	good	3	poor to very poor
7	good to fair	2	very poor
6	fair	1	extremely poor

Total exposure: 1,197,310 langleys (6 years real-time)

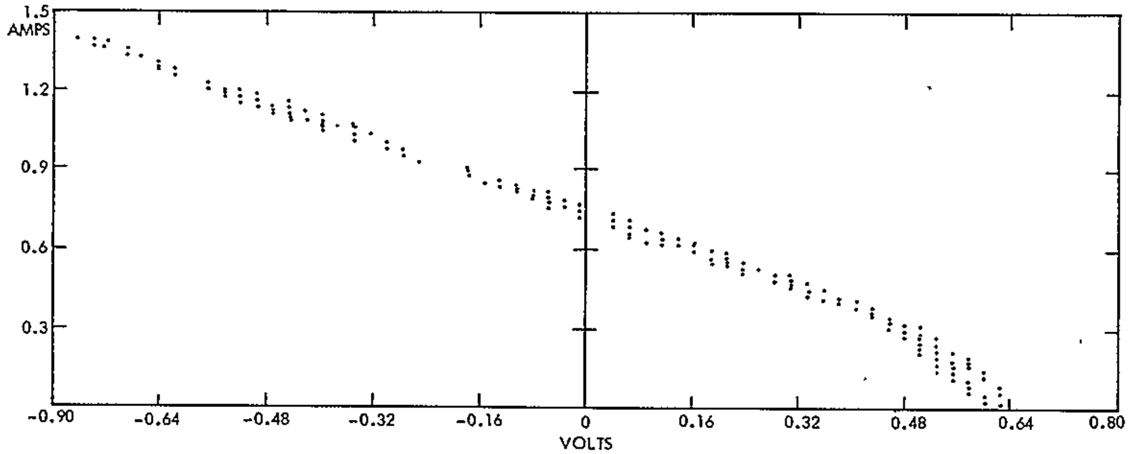

NORMALIZED DATA

Parameter	This Curve	Initial Curve*
V_{OC}	0.62 V	1.185 V
I_{SC}	0.73 A	1.334 A
$V_{P_{max}}$	0.43 V	0.900 V
$I_{P_{max}}$	0.39 A	1.222 A
P_{max}	0.17 W	1.09 W

Module DE440 (Type I) after failure in EEKQUA Test

220,138 langleys (6,695 langleys of UV)

*Initial curve from JPL LAPSS measurements.

a. EEKQUA: DE440 (Type I)

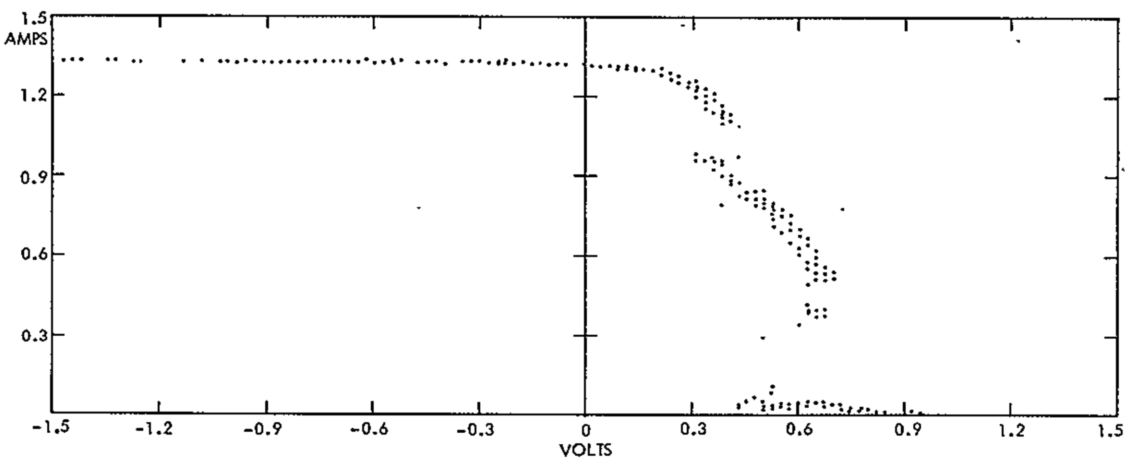

NORMALIZED DATA

Parameter	This Curve	Initial Curve
V_{OC}	--	1.125 V
I_{SC}	1.32 A	1.500 A
$V_{P_{max}}$	--	0.876 V
$I_{P_{max}}$	--	1.305 A
P_{max}	--	1.14 W

Module DE242 (Type V) after failure in 34° South Direct Rack Test

148,760 langleys (4,486 langleys of UV)

Note. Cell performance not a result of faulty instrumentation interconnect as was stated in the August report.

*Initial curve from JPL LAPSS measurements.

b. 34°S Rack: DE242 (Type V)

Figure 4-3. I-V Curves of Submodules Which Failed DSET EEKQUA and 34°S Rack Tests

C. FIELD EXPOSURE

1. Soiling

Electrical degradation of the modules undergoing field exposure was monitored through changes in maximum power output calculated from LAPSS I-V curves.

Two groups of curves were obtained: the first with the modules in the as-weathered condition; the second after they had been washed (cf. Section III.D). In reviewing the detailed results it can be seen that soiling is site-specific. Modules tested at JPL show maximum power outputs that are consistently 2%-6% higher (occasionally even more) after washing than they were in the as-weathered condition. The other sites show little or no difference. As a result of this observation, comparisons from site to site have been made on the basis of the maximum power developed by washed modules.

2. Performance

Figures 4-4 and 4-5 summarize the effects of field exposure on performance of minimodules and submodules, respectively; the data on which these graphs are based are presented in Appendix C. Each of the points plotted in Figure 4-4 corresponds to the average of the results for the particular test set if their scatter is not more than a few percent. An exception is Type I, where considerable scatter developed at the outset, and therefore individual results are plotted. (Only one Type X module was deployed at each of the three sites.)

Eight module types show essentially no change in maximum power over 500 to 700 days of field exposure. However, those that incorporate Super Dorlux (Types I and II) began to degrade early, and in a number of cases failure also occurred early--for example, relative maximum power outputs below 70% after less than 100 days exposure at JPL. This is again due to structural damage and shrinkage of the hardboard during module manufacture, followed by expansion toward its equilibrium length during exposure. The eventual result was cell cracking and power loss. One Type V minimodule at Pt. Vicente began to show power loss after 232 days of exposure, and one Type IX minimodule at Goldstone began to lose power after 77 days of exposure. Results of nondestructive failure analysis of selected modules are presented in Table 4-7. Weather data at the test sites are given in Figure 4-6.

Other changes have taken place in the modules that have not led to significant loss of maximum power output. At the JPL test site the following have been noted at the last examination of the minimodules:

(1) Cracking of Korad cover film over corner cell: DE101 (Type I) and DE132 (Type III)

(2) Widely-spaced crazing of Korad film: DE131 (Type III)

(3) Crazing of Tedlar cover film: MB110, MB111, and MB112 (Type IV)

(4) Delamination of encapsulant: CE110 and CE111 (Type VI)

(5) Tarnish and occasional small corrosion spots on photovoltaic circuit: PW104, PW105, and PW106 (Type XI) and SE101 and SE102 (Type IX)

(6) Darkening of encapsulant near sealant: all DE modules (Types I, III, and V), all MB modules (Type IV) (intense), and the GE module, GE102 (Type X)

ORIGINAL PAGE IS
OF POOR QUALITY

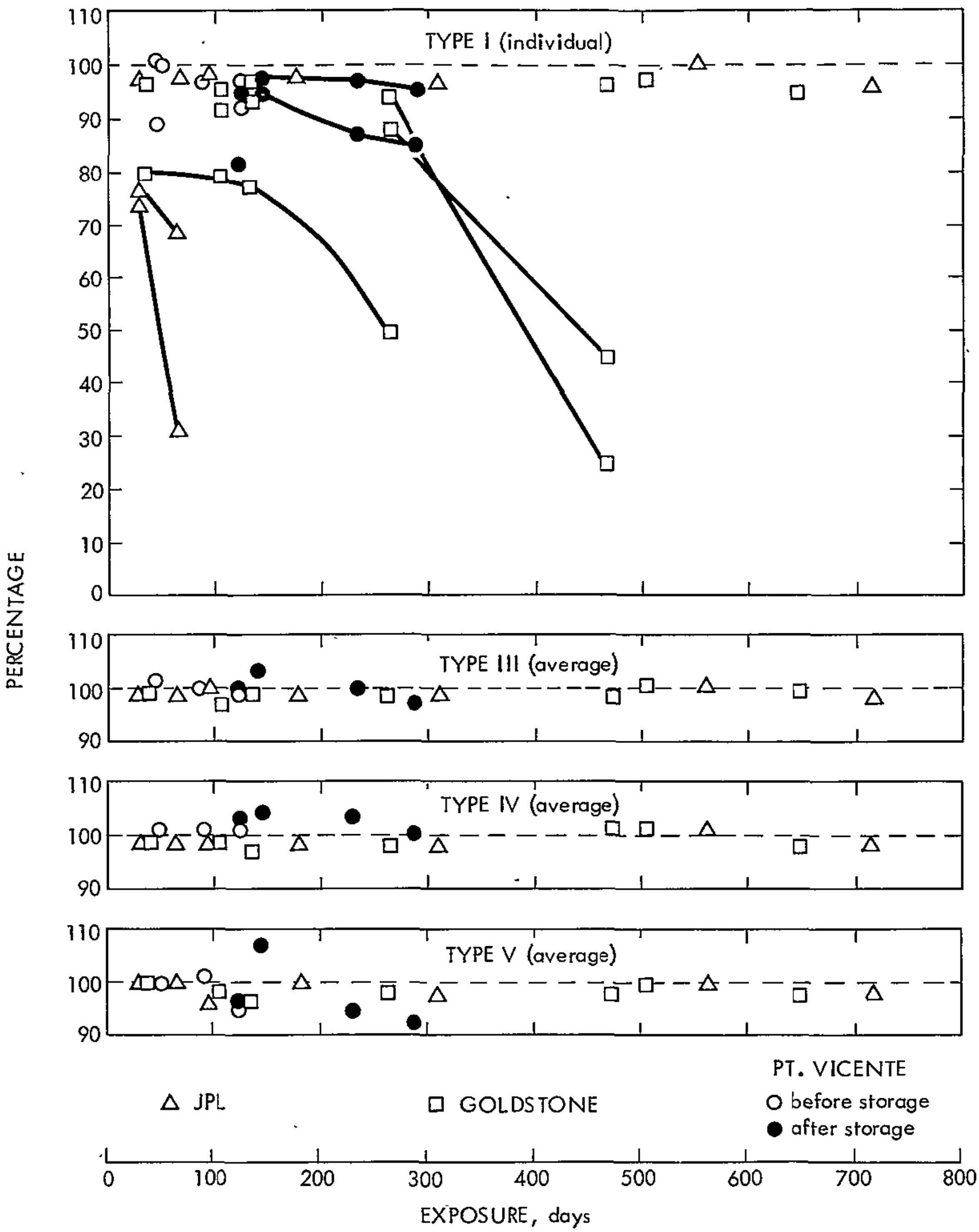

Figure 4-4. Minimodule Field-Test Results: Percentage of Initial Maximum Power Output Retained After Cleaning

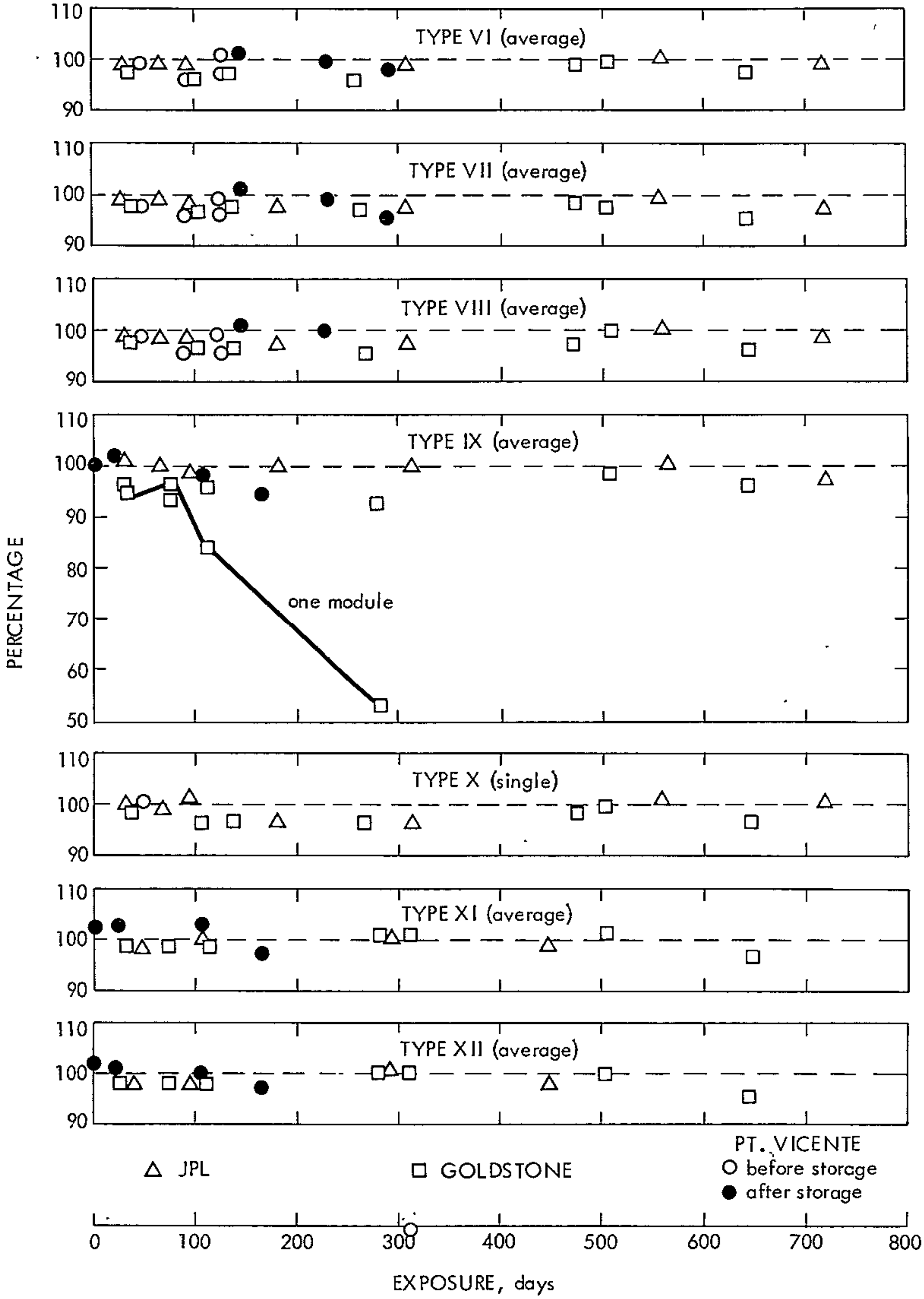

Figure 4-4. Minimodule Field-Test Results: Percentage of Initial Maximum Power Output Retained After Cleaning (cont'd)

ORIGINAL PAGE IS
OF POOR QUALITY

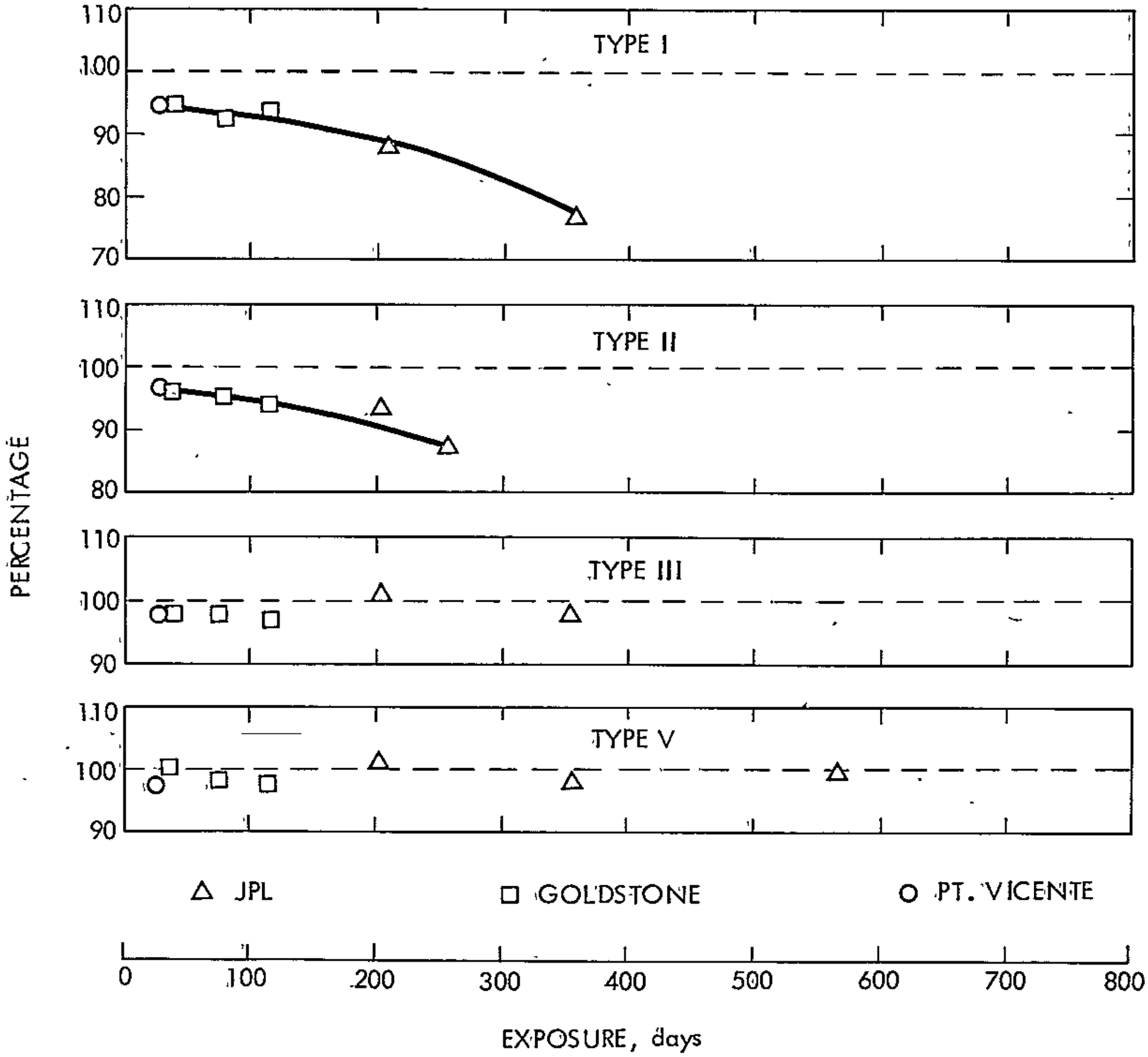

Figure 4-5. Submodule Field-Test Results: Percentage of Initial Maximum Power Output Retained After Cleaning

Table 4-7. Results of Failure Analyses of Field-Tested Modules

	Serial Number	Exposure, days	Date Removed	Site	Problem	Cause	Type
Minimodules	DE102	63	9/29/80	JPL	P_{max} 6.33 to 4.35 W	Cell cracked during washing	I
	DE103	63	9/29/80	JPL	P_{max} 6.33 to 1.98 W	Cell cracked during washing	I
	DE104	473	2/19/82	Goldstone	P_{max} 6.21 to 1.67 W	Cracked cell	I
	DE105	138 473	2/24/81 2/19/82	Goldstone Goldstone	P_{max} 6.47 to 5.12 W P_{max} 6.47 to 2.88 W	Cracked cell Cracked cell	I
	DE107	48	12/18/80	Pt. Vicente	P/P_o 0.98 before wash 0.89 after	Cells cracked during washing	I
Submodules	DE362	215	10/29/81	Goldstone	$P_{max} = 0$	Cracked cell	III
	DE419	353	9/16/81	JPL	$P_{max} = 0$	Cracked cell	I
	DE426	201	2/23/81	JPL	$P_{max} = 0$	Cracked cell	I
	DE430	353	9/16/81	JPL	$P_{max} = 0$	Cracked cell	I
	DE433	201	2/6/81	JPL	P_{max} 1.28 to 0.46 W	Cracked cell	I
	DE550	215	10/29/81	Goldstone	$P_{max} = 0$	Cracked cell	II
	DE556	35	3/17/81	Goldstone	P/P_o 0.80 before wash 0 after	Cracked cell	II
	SE120	279	2/19/82	Goldstone	P_{max} 9.75 to 5.13 W	Interconnect	IX

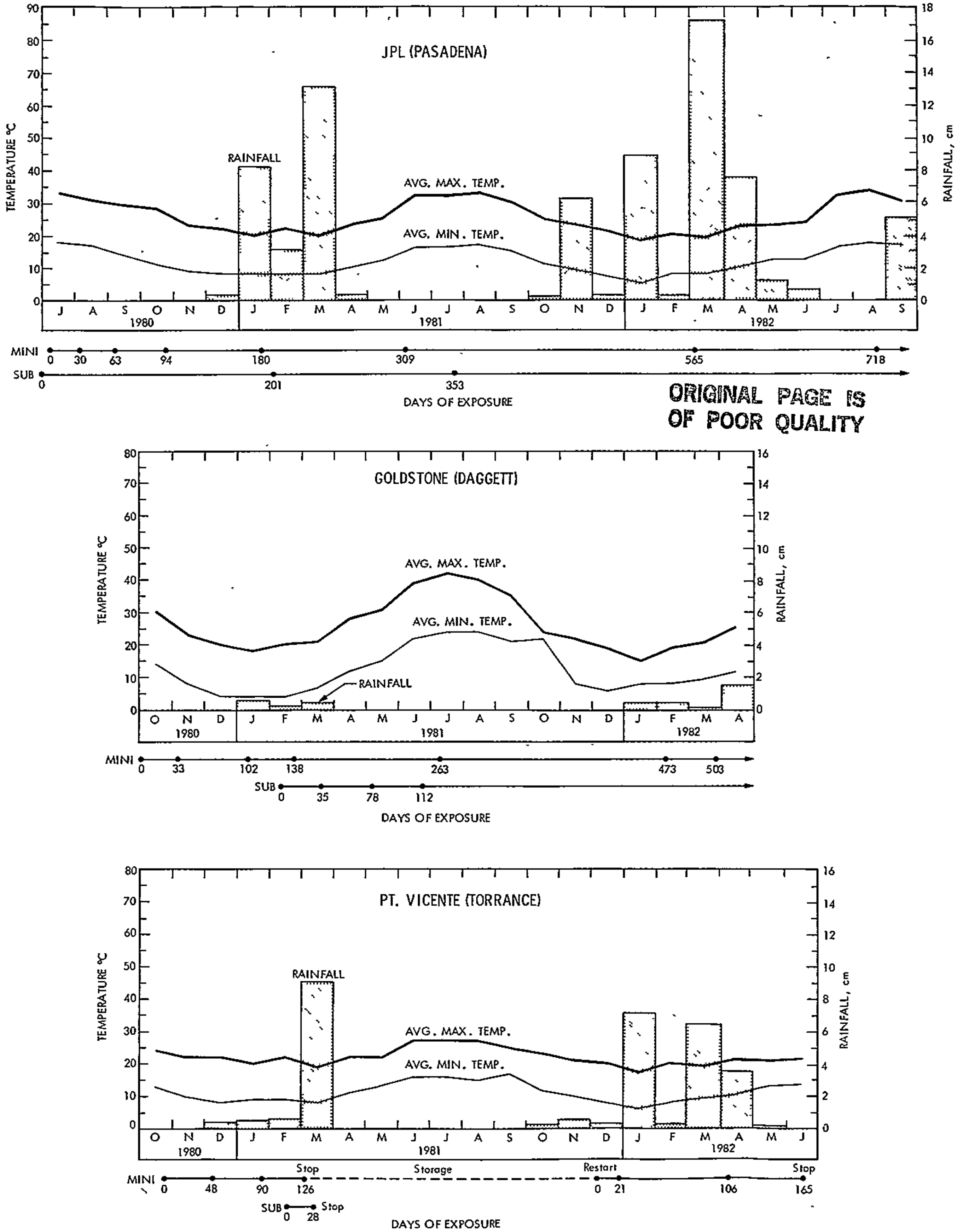

Figure 4-6. Temperature and Precipitation at Test Sites (measuring station in parentheses)

SECTION V

DISCUSSION

Even though this field testing program has been in progress for only a short time compared with the intended 20-year life of commercial modules, several interesting observations have been made. For the most part, little degradation of maximum power output has occurred in modules other than Types I and II, which incorporate Super Dorlux, and Type IX, in which the cells are electrostatically bonded to type 7070 borosilicate glass.

The failures of Types I and II modules result primarily from the manufacturing process used to laminate the hardboard panel between layers of EVA. This was accomplished by a standard vacuum-bagging operation in which a temperature of 150°C was required to cure the plastic. As a result of these conditions, steam was generated from the moisture normally present in the hardboard, and voids, blisters, and cracks were sometimes produced. In addition, the hardboard shrank by 0.25% as the water was pumped out of it. During field exposure water slowly diffused back into the hardboard, causing it to expand. The solar cells were placed in tension by this seemingly slight expansion, and some broke (Reference 6). A new manufacturing process calls for pre-coating both sides of the hardboard at room temperature with adhesive-bonded white plastic film and then adhesive-bonding the encapsulated cell string to the sandwich. Calculations indicate that such a technique will produce a substrate insensitive to humidity fluctuations with time constants less than a year.

The Type IX modules have been found to be quite easily degraded during laboratory testing. Two were subjected to temperature and humidity-freeze cycle testing; both glass superstrates cracked, implying that cells also cracked, and one of the modules lost electrical continuity. The hail-test module cracked at all four of the lowest-velocity impacts; the cover of the DSET SuperMaq module cracked early in testing. During field exposure the modules fared rather better: output of the two modules at JPL remain essentially unchanged after two years; two of the three at Goldstone are essentially unchanged after ten months, while one failed after nine months; the three at Pt. Vicente may have degraded slightly after five months.

There are two main causes of failure in Type IX modules. First, edge flaws may initiate cracks in the glass superstrate, even though it is reported to be stronger than window glass; since the solar cells are bonded directly to the glass, they crack along with it. Second, it has apparently been difficult to achieve good electrical bonding of the interconnects to the cells. Slight motions can therefore lead to increased contact resistance or even to loss of continuity altogether.

Soiling of all module Types, measured by the increase in maximum power output after washing, seems to be slightly greater at the JPL Pasadena site than at Goldstone or Pt. Vicente (Appendix E). There appears to be a fairly consistent change of 2%-4% for the JPL modules, while the others are generally unchanged. This is consistent with other results obtained by exposure of various modules (Reference 7).

Prior exposure tests (performed by W. Neiderheiser and C. Maag of JPL) on specimens of various materials showed somewhat greater degradation than has been observed here. Those specimens were not incorporated in modules, but were mounted in test frames which allowed aerodynamic flutter. This mechanical flexure, together with abrasion by airborne sand not encountered in the present testing, seems to account for much of that enhanced degradation. Particularly affected by these processes were Korad, which crazed, and Tedlar, which was enbrittled. In addition, RTV silicone rubbers were eaten or other-wise destroyed by birds, a relatively common problem which has not been encountered with the materials of the present substrate modules.

Otherwise, there is little difference to date between modules employing glass superstrates and those with low-cost structural substrates. Similarly, there is little difference in maximum power output among modules employing EVA, polyurethane, or RTV silicone rubber as pottants. Whether Mylar, Acmetité, or aluminium foil is used as a back cover makes little difference as yet.

REFERENCES

1. Block V Solar Cell Module Design and Test Specifications for Intermediate Load Applications - 1981, JPL Internal Document No. 5101-161, Jet Propulsion Laboratory, Pasadena, California, February 20, 1981.

2. Moore, D. and Wilson, A., Photovoltaic Solar Panel Resistance to Simulated Hail, JPL Document No. 5101-62, DOE/JPL-1012-78/6, Jet Propulsion Laboratory, Pasadena, California, October 15, 1978.

3. Zerlaut, G. A., Anderson, T. E. and Arnett, J. C., "Accelerated Weathering of Photovoltaic Modules Employing Natural Sunlight," Proceedings of the 27th Annual Meeting, Institute of Environmental Sciences, p. 51, 1981.

4. Griffith, J. S., Environmental Testing of Block III Solar Cell Modules/Part I: Qualification Testing of Standard Production Modules, JPL Publication 79-96, JPL Document No. 5101-134, DOE/JPL-1012-30, Jet Propulsion Laboratory, Pasadena, California, September 1, 1979.

5. Smokler, M. I., User Handbook for Block IV Silicon Solar Cell Modules, JPL Publication 82-73, JPL Document No. 5101-214, DOE/JPL-1012-75, Jet Propulsion Laboratory, Pasadena, California, September 1, 1982.

6. Carroll, W., Coulbert, C., Cuddihy, E., Gupta, A., and Liang, R., Photovoltaic Module Encapsulation Design and Materials Selection: Volume 1, JPL Publication 81-102, JPL Document No. 5101-177, DOE/JPL-1012-60, Jet Propulsion Laboratory, Pasadena, California, November 1, 1981.

7. Hoffman, A. R., Maag, C. R., Photovoltaic Module Soiling Studies, May 1978 - October 1980, JPL Publication 80-87, JPL Document No. 5101-131, DOE/JPL-1012-49, Jet Propulsion Laboratory, Pasadena, California, November 1, 1980.

APPENDIX A

DESCRIPTION OF MATERIALS USED IN MODULE FABRICATION

Acmetite	One-mil aluminum foil coated on both sides with 0.5 mil polyester film. No longer being produced. Supplier: Acme Backing Corporation, Stamford, CT 06977
Acrylic transfer adhesive	Supplier: National Starch & Chemical Corp., 10 Finderne Ave., Bridgewater, NJ 08807
Craneglas	A nonwoven fiberglass web. In this case, 7-mil thick type 230 Craneglas, consisting of DE glass fibers (lime aluminoborosilicate) nominally 6.25 μm in diameter with a partially-hydrolyzed polyvinyl acetate binder. (This material provides an air path during vacuum bagging, contributes to dielectric properties, and can be used as a carrier for EVA.) Supplier: Crane & Co., Inc., Dalton, MA 01226
EVA	A copolymer of ethylene and vinyl acetate. White EVA is pigmented with titanium and zinc oxides. Supplier: Springborn Laboratories, Inc., Enfield, CT 06082.
GRC	Glass-fiber reinforced concrete produced by double spraying of concrete around a central stream of 1-in. (2.5-cm) long fibers chopped from Corning alkaline-resistant glass roving. Supplier: MBAssociates, Box 196, San Ramon, CA 94583
Korad	A modified multipolymer ultraviolet-screening acrylic film, here type 212. Supplier: Georgia-Pacific, Polymer Materials Division, 290 Ferry St., Newark, NJ 07105
Mylar	A polyester film (polyethylene terephthalate), here type A. Supplier: E.I. DuPont de Nemours & Co., Inc., Wilmington, DE 19898
Primer	Z-6030, a mixture of methacryloxy-propyl-trimethoxysilane and N,N-dimethylbenzamine in a solvent. Supplier: Dow-Corning Corp., Midland, MI 48640

Q-621/626 Polyurethane	A Q-thane 100%-solids aliphatic prepolymer and polyol system. Supplier: K.J. Quinn & Co., Inc., 195 Canal St., Malden, MA 02148.
RTV Silicone Rubber	GE 534-044, an experimental material never produced commercially. Supplier: General Electric Silicone Products Department, Waterford, NY 12188
Solar cell assemblies	Four manufacturers have supplied the assemblies used in the twelve module types:

Type IV

ARCO Solar, Inc., 20554 Plummer St., Chatsworth, CA 91311

Phosphorus is diffused into the front surface of boron-doped silicon to form the junction. The front metallization and back contact pads are printed silver; the rest of the back metallization is aluminum. No antireflective coating is used. Interconnects are solder-coated copper ribbon.

Types VI, VII, VIII, X, XI, and XII

ASEC (Applied Solar Energy Corp.), 15251 E. Don Julian Road, City of Industry, CA 91749

The metallization consists of layers of titanium, palladium, and silver (outward from the silicon). The cells in the Types VI, VII, VIII, and X Modules have an SiO antireflective coating; cells in the Types XI and XII Modules have none. Interconnects are copper ribbon coated with 60/40 solder, which is reflowed for assembly.

Types I, II, III, and V

Solar Power Corp., 20 Cabot Road, Woburn, MA 01801

The metallization and antireflective coating are considered confidential. A 60/40 solder dip is applied to the metallization. The interconnects are solder-plated oxygen-free dead-soft annealed copper.

	Type IX
	Spire Corp., Patriots Park, Bedford, MA 01730
	The cells are ion-implanted with phosphorus on the front and boron on the back. The metallization is a photolithographic pattern of titanium, palladium, and silver layers outward from the silicon. The antireflective coating is titania. Interconnects are copper mesh with a proprietary coating which is then solder-covered; they are reflow-soldered to the cells.
Sunadex glass	A virtually iron-free glass with high energy transmission; one side is lightly patterned.
	Supplier: ASG Industries, Inc., Box 929, Kingsport, TN 37662
Super Dorlux	A natural-bonded wood-fiber product tempered with linseed oil.
	Supplier: Masonite Corporation, 29 N. Wacker Dr., Chicago, IL 60606
Tedlar	Code 100BG30UT, a polyvinyl fluoride film 1.0 mil (25 μm) thick, both sides adherable (surface roughened), glossy, medium tensile strength and elongation, ultraviolet screening, and transparent.
	Supplier: E.I. DuPont de Nemours & Co, Inc., Wilmington, DE 19898.
3M Sealer XA-5376	A polyisobutylene solid sealer with a permanent polyethylene liner.
	Supplier: 3M Company, 3M Center, St. Paul, MN 55101
7070 glass	A borosilicate glass with a coefficient of thermal expansion similar to that of silicon.
	Supplier: Corning Glass Works, Corning, NY 14830

APPENDIX B

DETAILS OF MODULE CONSTRUCTION

B.1 TYPES I, II, III, AND V (Springborn Laboratories, Inc.)

<u>Types I, II, and III processing description</u>:

(1) Cut Super Dorlux or galvanized steel, Craneglas, EVA (clear and white), and Korad or Tedlar to size.

(2) Clean the substrate, Solar Power cell assembly, and cover film with isopropyl alcohol.

(3) Apply primer to the cleaned surfaces.

(4) Place the Craneglas on the substrate.

(5) Place the white EVA on the Craneglas.

(6) Locate the solar cell assembly face up on the white EVA.

(7) Place the clear EVA on the cells.

(8) Place the cover film on the clear EVA.

(9) Place the assembly in a vacuum chamber which contains a diaphragm.

(10) Apply a vacuum on both sides of the diaphragm for five minutes.

(11) Bleed off the vacuum on one side of the diaphragm, but maintain the vacuum on the module.

(12) Cure for 15 minutes at 300°F (150°C).

(13) Cool under vacuum.

<u>Type V processing description</u>:

Type V is assembled and cured in a similar fashion except that a superstrate in employed; the order of component assembly is therefore reversed and the cells are placed face down.

TYPE I

DE 101 - 115
DE 401 -490

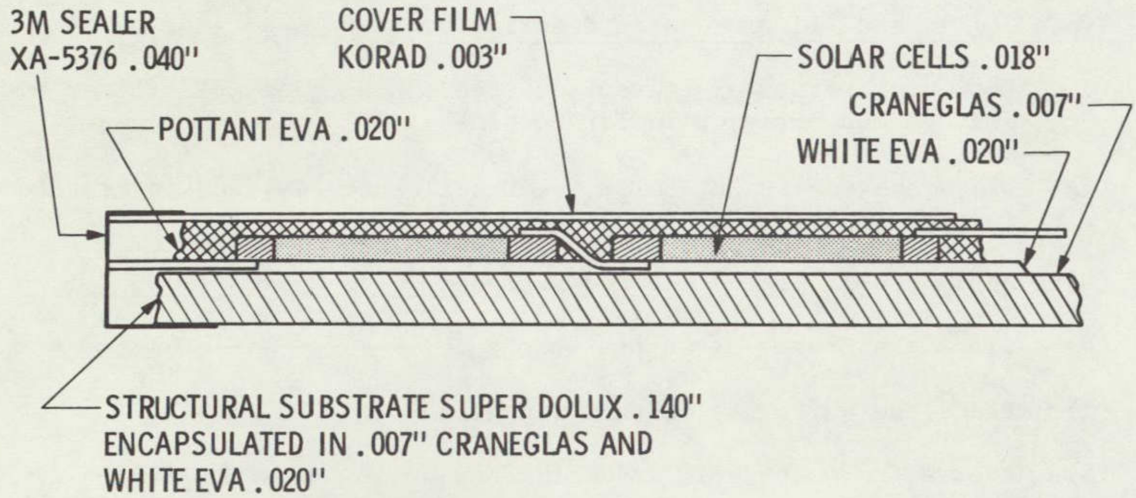

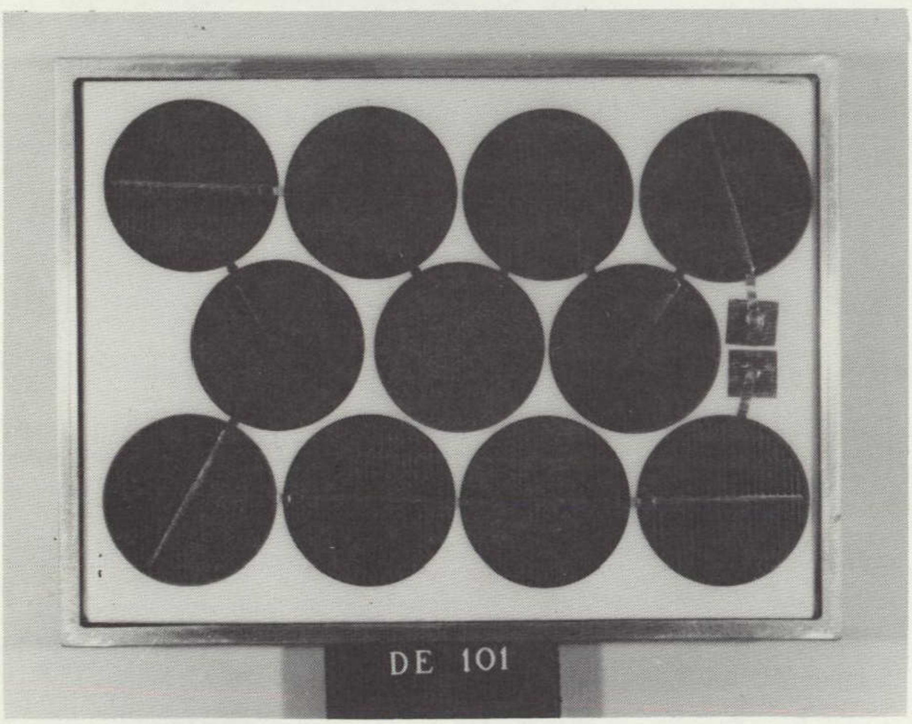

Type I

TYPE II
DE 501 - 590

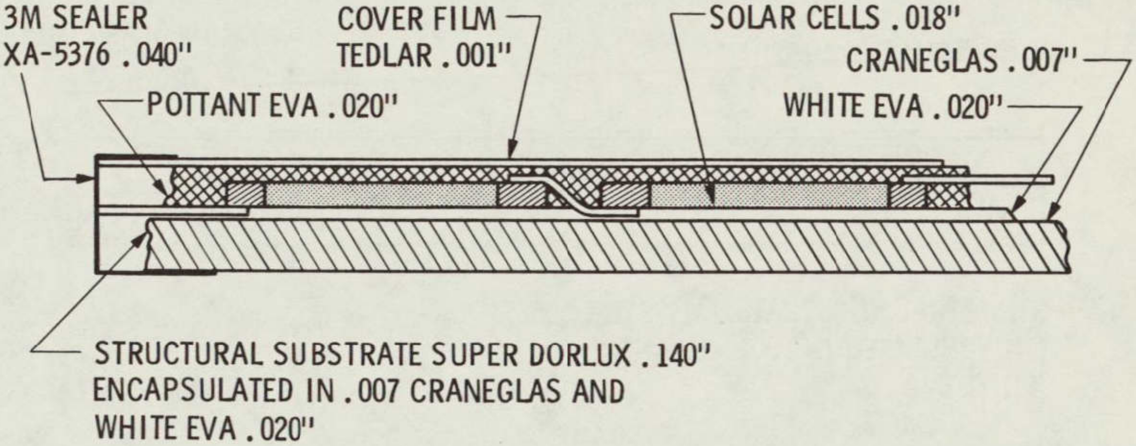

TYPE III

DE 131 - 145
DE 301 -390

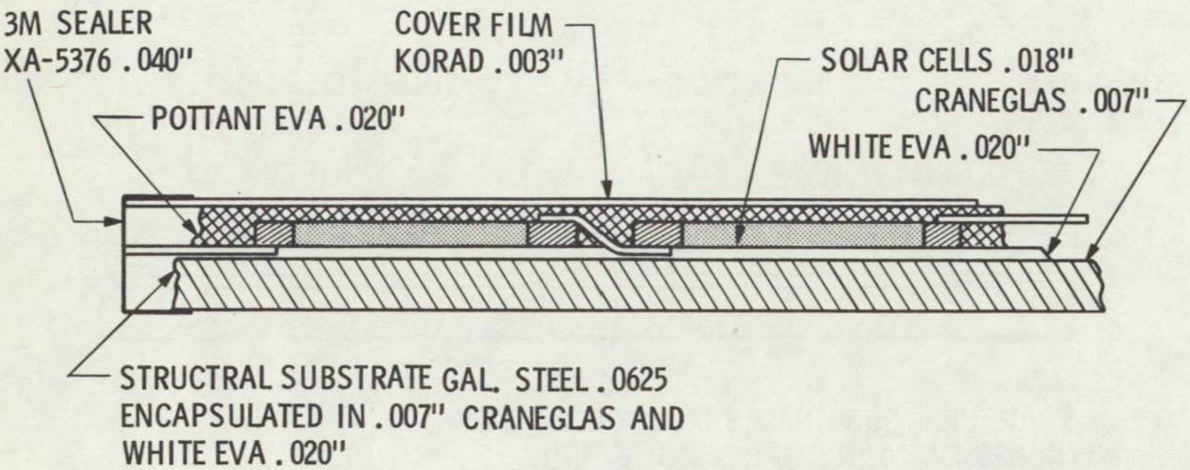

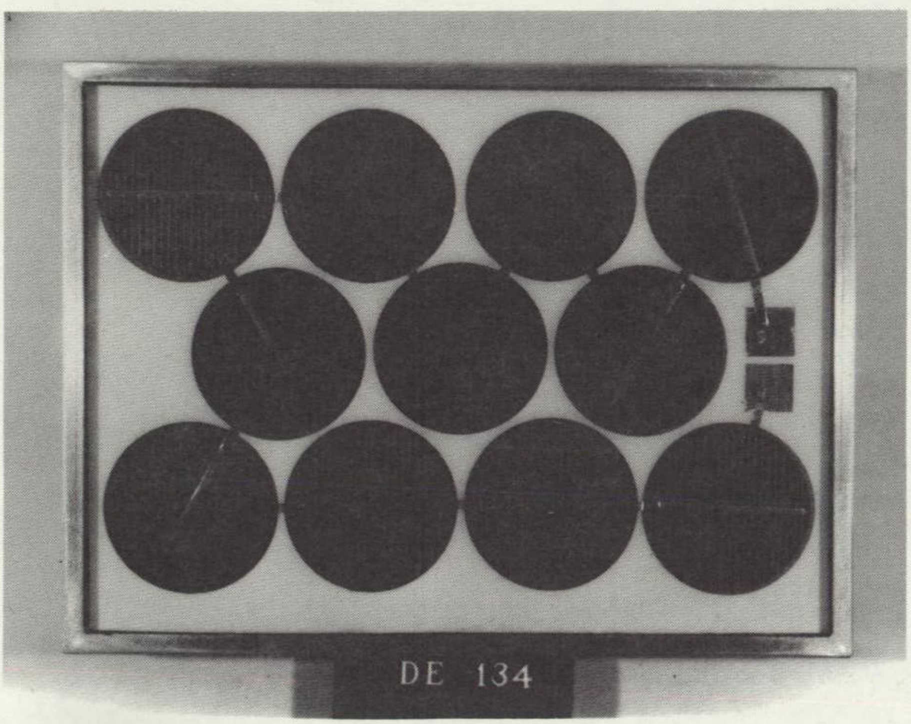

Type III

TYPE V

DE 116 - 130
DE 201 - 290

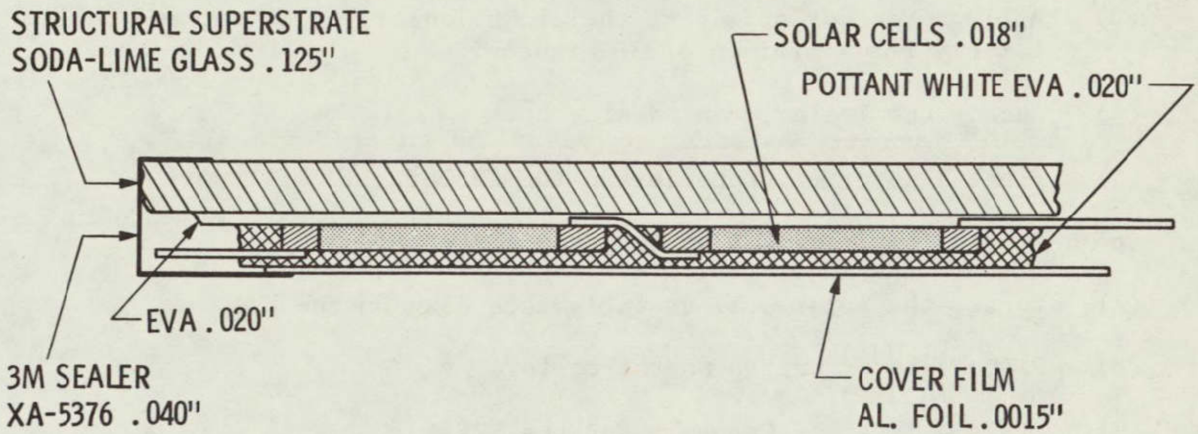

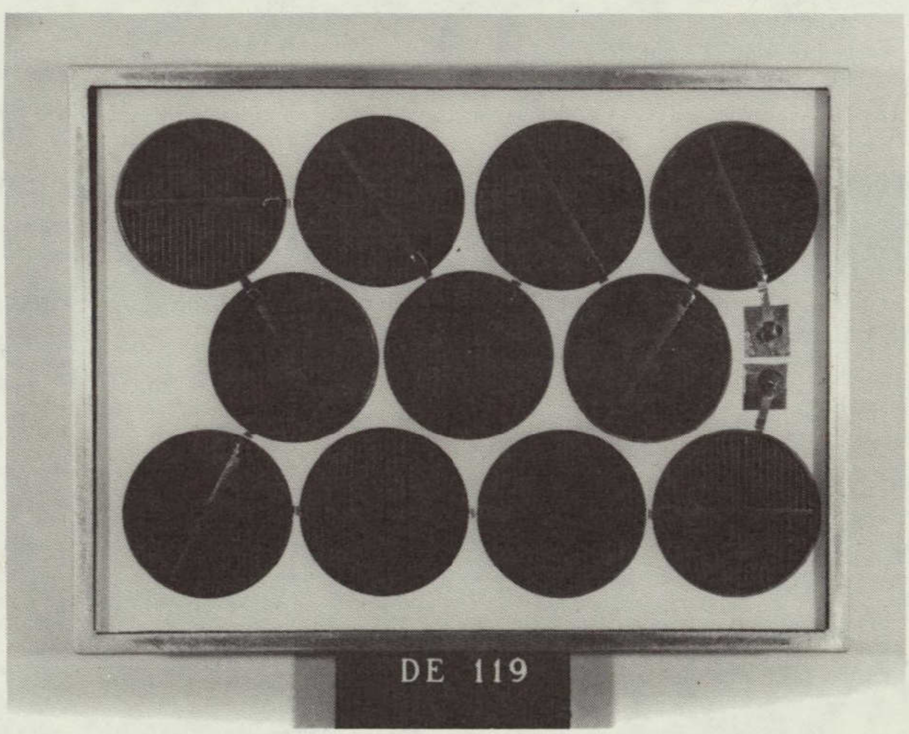

Type V

B.2 TYPE IV (MBAssociates)

Processing description:

(1) Cut the EVA, Craneglas, and Acmetite to size.

(2) Clean one side of the Tedlar and Acmetite and the entire ARCO Solar cell assembly with isopropyl alcohol.

(3) Apply a coat of primer to the clean Tedlar, Acmetite, and cells. Let dry for a minimum of 30 minutes.

(4) Anchor the Tedlar, coated side up.

(5) Place a layer of Craneglas on the Tedlar.

(6) Place a layer of EVA on the Craneglas.

(7) Locate the solar cell assembly face down on the EVA.

(8) Place a layer of EVA on the cells.

(9) Place a layer of Craneglas on the EVA.

(10) Place the Acmetite on the Craneglas.

(11) Vacuum bag the assembly.

(12) Heat to 120°F (50°C).

(13) Apply vacuum slowly: 10 minutes to 28.5 in. (72 cm) of Hg.

(14) Raise the temperature to 270°F (130°C) and cure for 30 minutes.

(15) Cool to 130°F (55°C), then release vacuum.

(16) Attach the module to the fiberglass-reinforced concrete substrate with acrylic transfer adhesive.

TYPE IV

MB 110 - MB 124

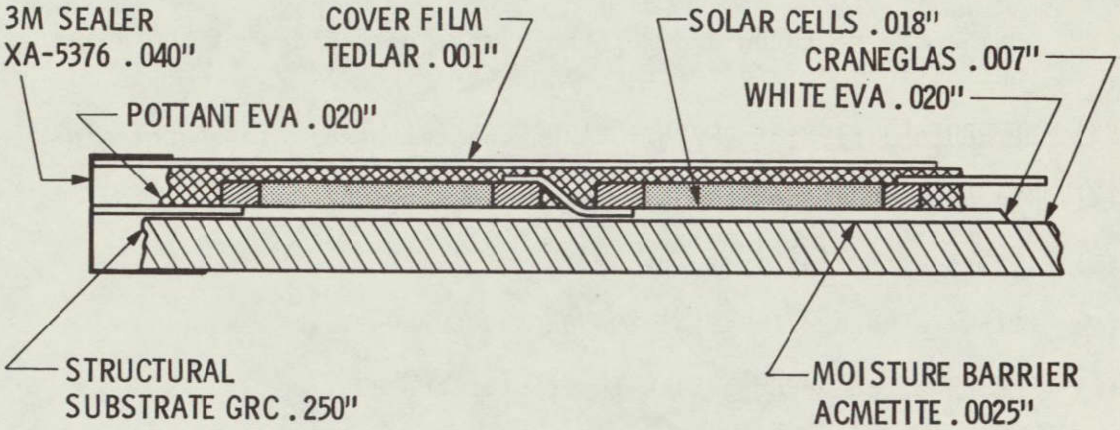

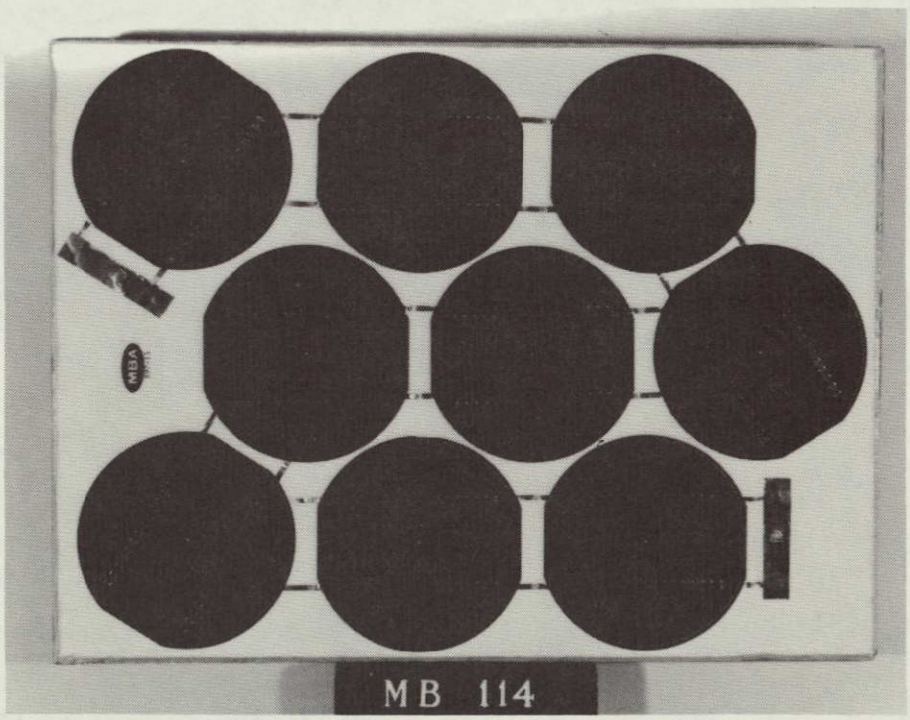

Type IV

B.3 TYPES VI, VII, AND VIII (Applied Solar Energy Corp.)

Processing description:

(1) Cut the glass, EVA, Craneglas, and Acmetite to size.

(2) Clean the glass, ASEC solar cell assembly, and Acmetite with isopropyl alcohol.

(3) Prime the textured side of the glass, both sides of the solar cells, and one side of the Acmetite.

(4) Place the first layer of EVA on the textured side of the glass.

(5) Locate the solar cell assembly face down on the EVA.

(6) Place Craneglas over the cells.

(7) Place a second layer of EVA on the Craneglas.

(8) Place a second Craneglas layer over the EVA.

(9) Place the Acmetite film on the Craneglas.

(10) Place in a vacuum bag and evacuate for 10 minutes.

(11) Cure for 15 minutes at 300°F (150°C).

TYPE VI
CE 101 - 115

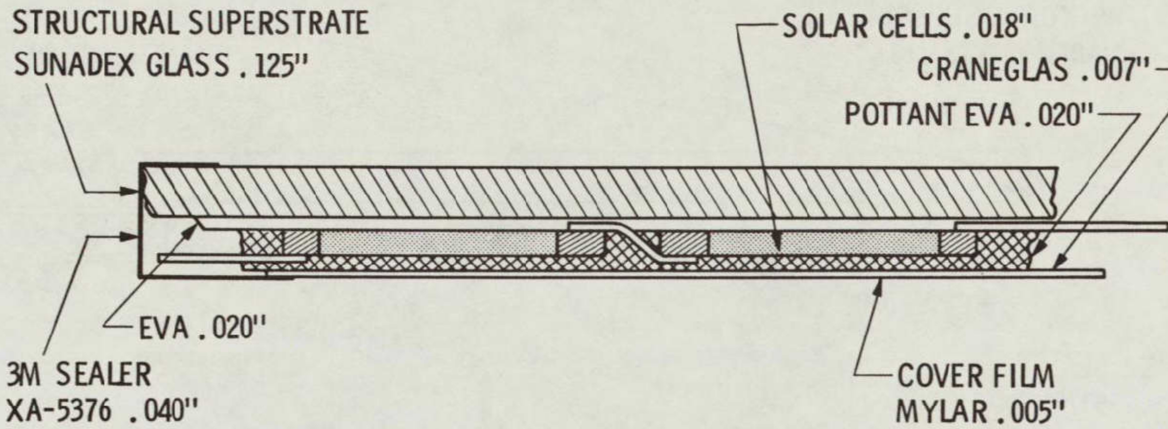

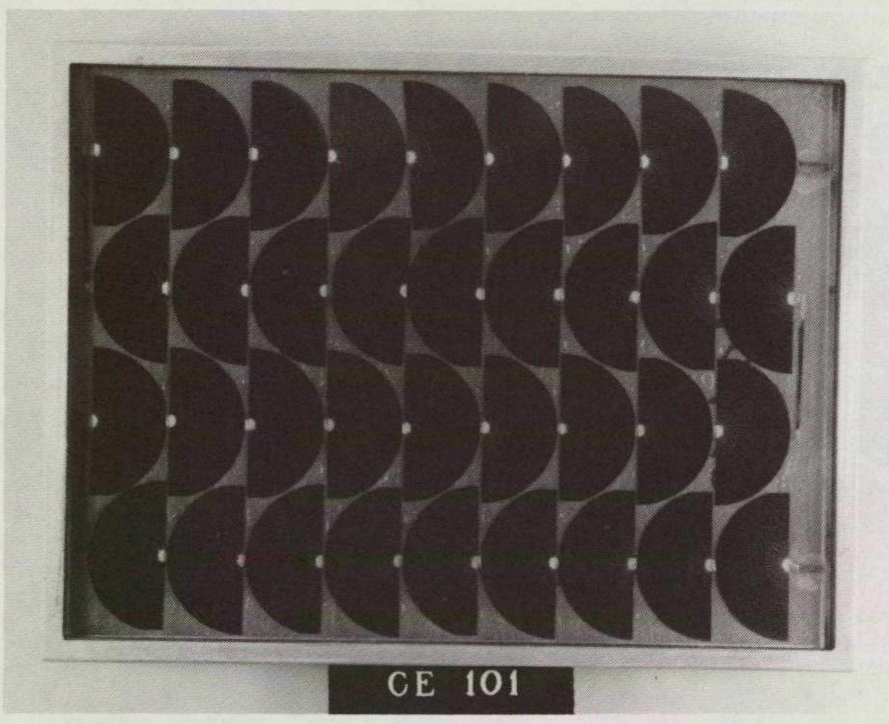

Type VI

TYPE VII
CE 116 - 130

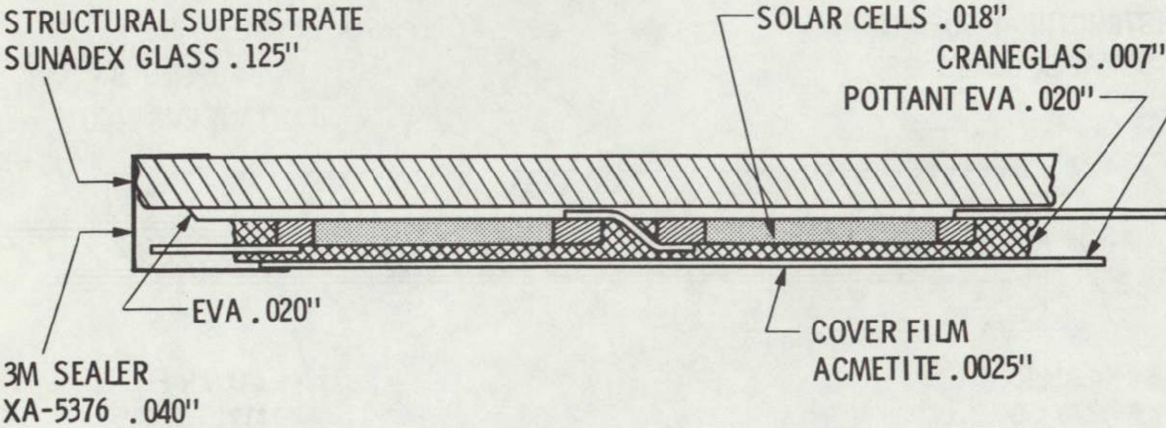

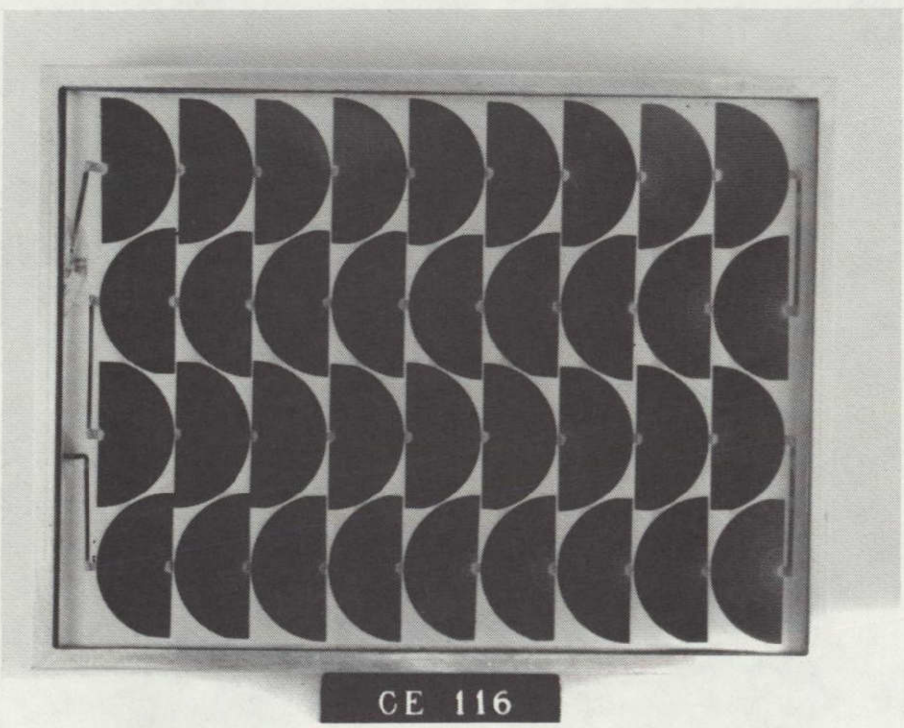

Type VII

TYPE VIII
CE 131 - 145

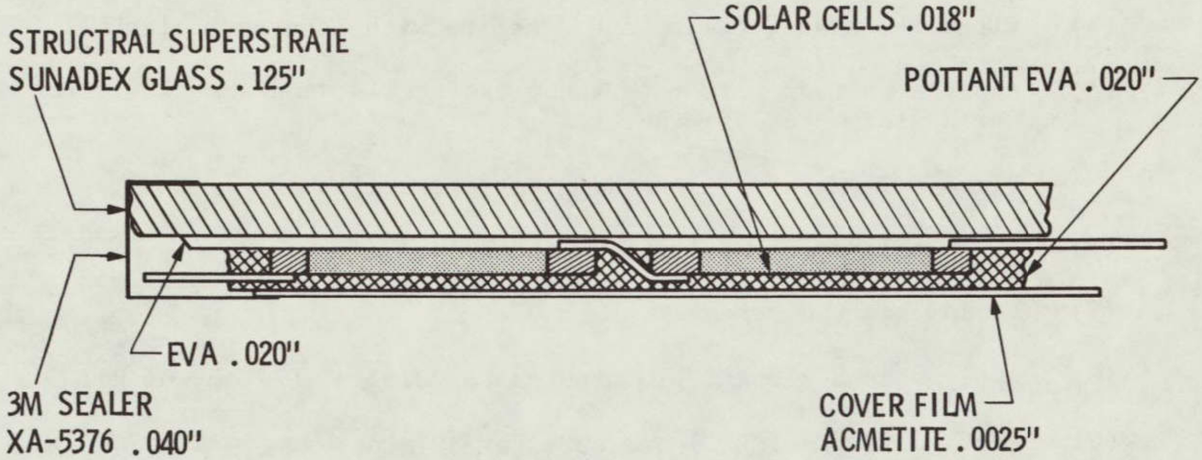

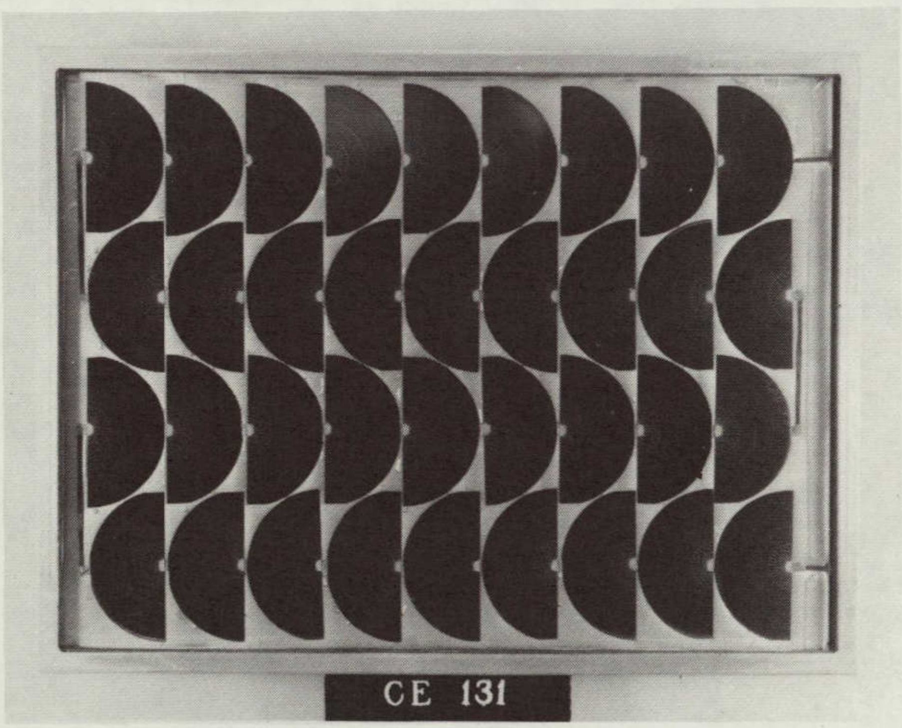

Type VIII

B.4 TYPE IX (Spire Corporation)

Processing description:

(1) Electrostatically bond the Spire solar cell assembly to the glass.

(2) Cut EVA and Acmetite to size.

(3) Clean the glass, cells, and Acmetite with isopropyl alcohol.

(4) Apply a coat of primer to the glass, cells, and Acmetite. Let dry for a minimum of 30 minutes.

(5) Place a layer of EVA on the glass and cells.

(6) Place a layer of Acmetite on the EVA.

(7) Vacuum bag the assembly.

(8) Apply vacuum slowly: 10 minutes to 28.5 in. (72 cm) of Hg.

(9) Heat to 270^{o}F (130^{o}C) and cure for 30 minutes.

TYPE IX
SE 101 - SE 110
SE 120 - SE 124

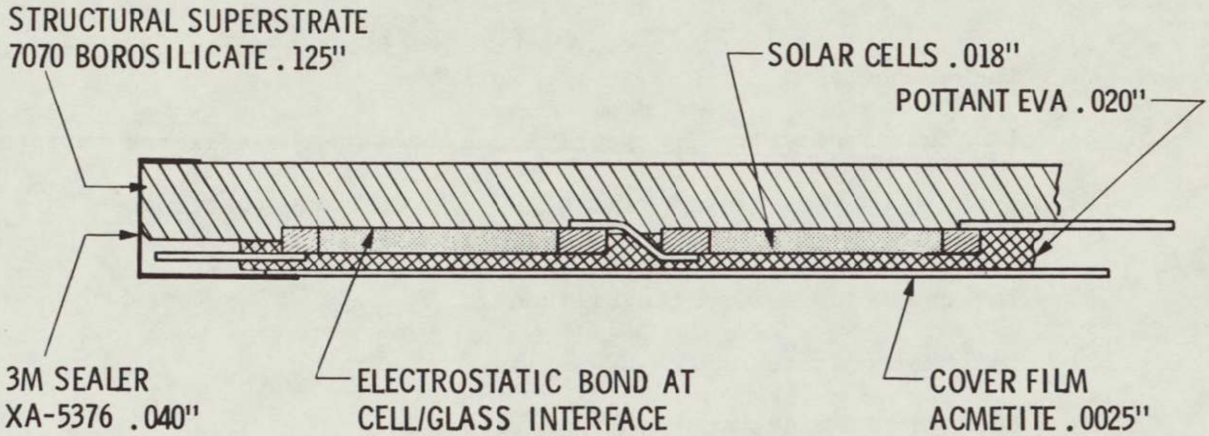

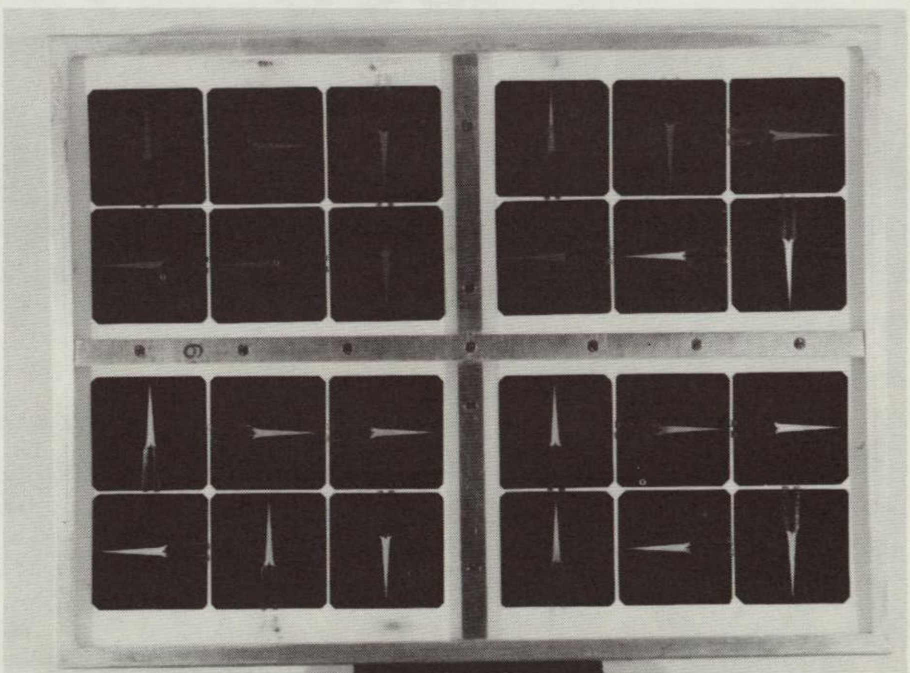

Type IX

B.5 TYPE X (General Electric Company)

Processing description:

(1) Cut glass, Craneglas, and Acmetite to size.

(2) Clean the glass, Acmetite, and ASEC solar cell assembly with isopropyl alcohol.

(3) Spray a thin film of deaerated GE RTV silicone rubber 534-044 on the Craneglas.

(4) Locate the solar cell assembly face down on the silicone surface.

(5) Spray 0.040-in. (1-mm) film of GE RTV silicone rubber 534-044 on the backs of the cells.

(6) Lay the Craneglas on the silicone.

(7) Lay the Acmetite on the Craneglas.

(8) Cure for 24 hours at room temperature.

TYPE X
GE 101 - GE 105

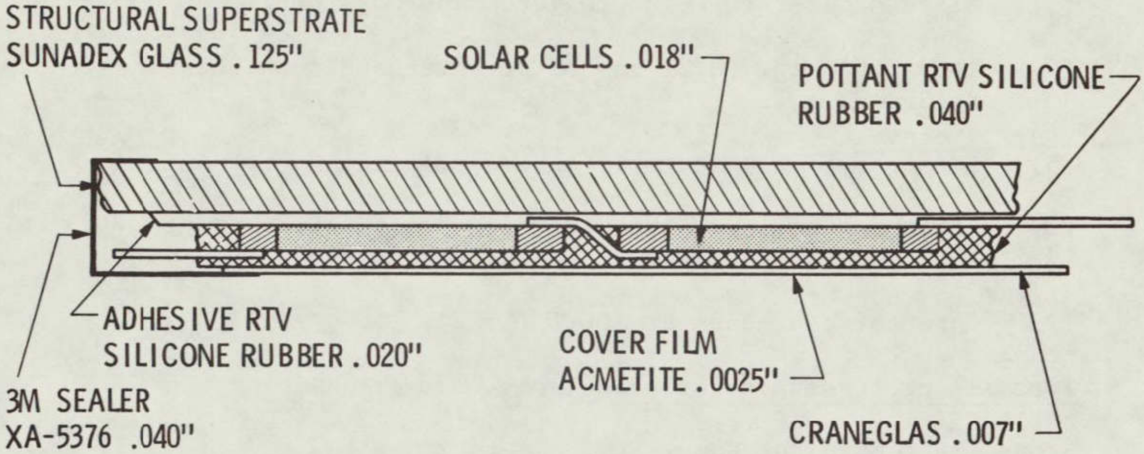

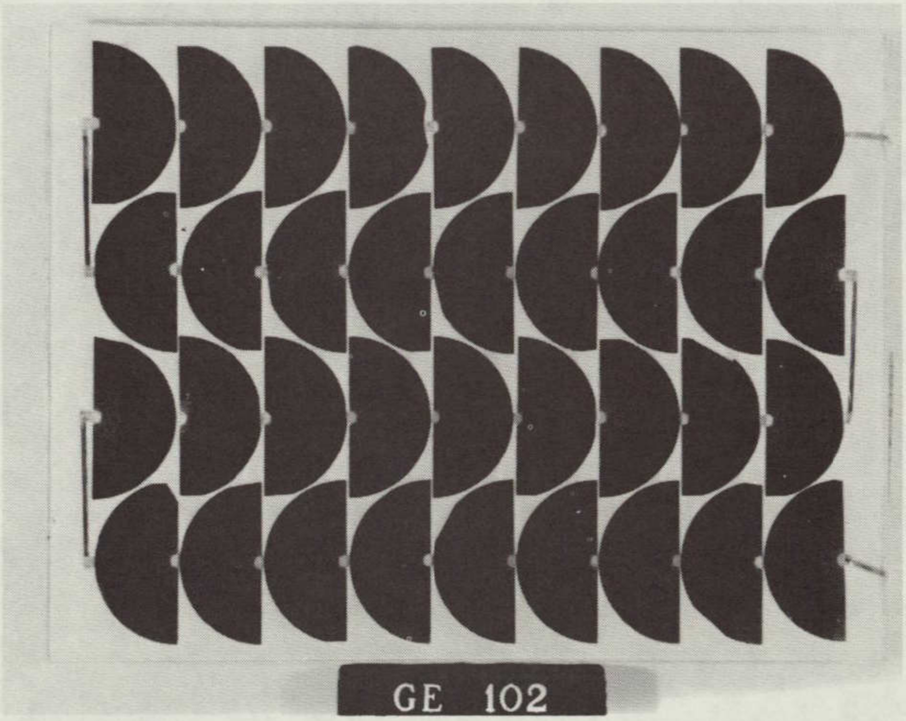

Type X

B.6 TYPES XI AND XII (Photowatt International, Inc.)

Type XI Processing description:

(1) Cut glass to size.

(2) Clean the glass and ASEC solar cell assembly with isopropyl alcohol.

(3) Mix and deaerate Quinn polyurethane Q621/626.

(4) Pour 0.010 in. (0.25 mm) of polyurethane onto the glass (no primer required).

(5) Locate the cell assembly on the polyurethane.

(6) Cover the cells to the desired pottant thickness of 0.125 in. (3.2 mm) with additional polyurethane.

(7) Cure for two hours at 200°F (93°C).

Type XII processing description:

Steps 1-6 remain the same.

(7) Place precut and cleaned Acmetite on polyurethane.

(8) Cure for two hours at 200°F (93°C).

TYPE XI

PW 101 - PW 115

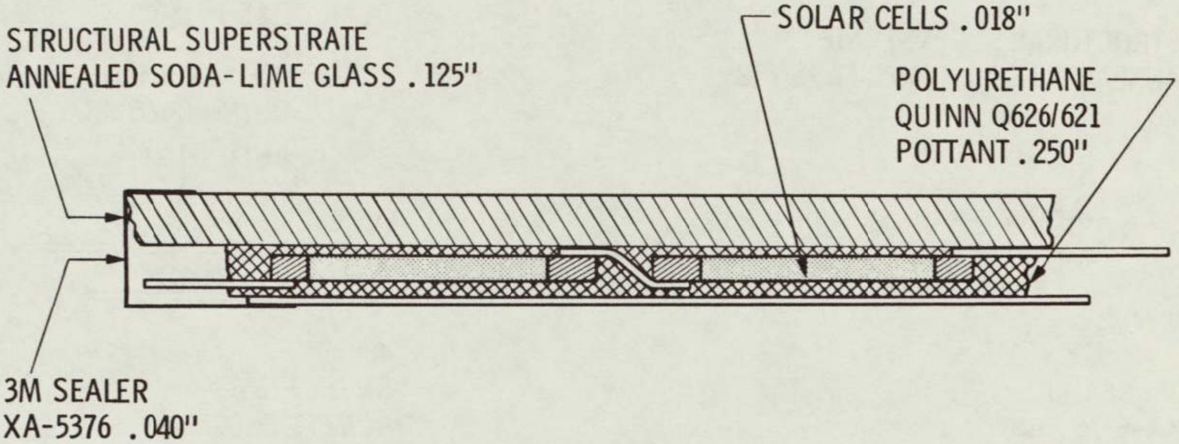

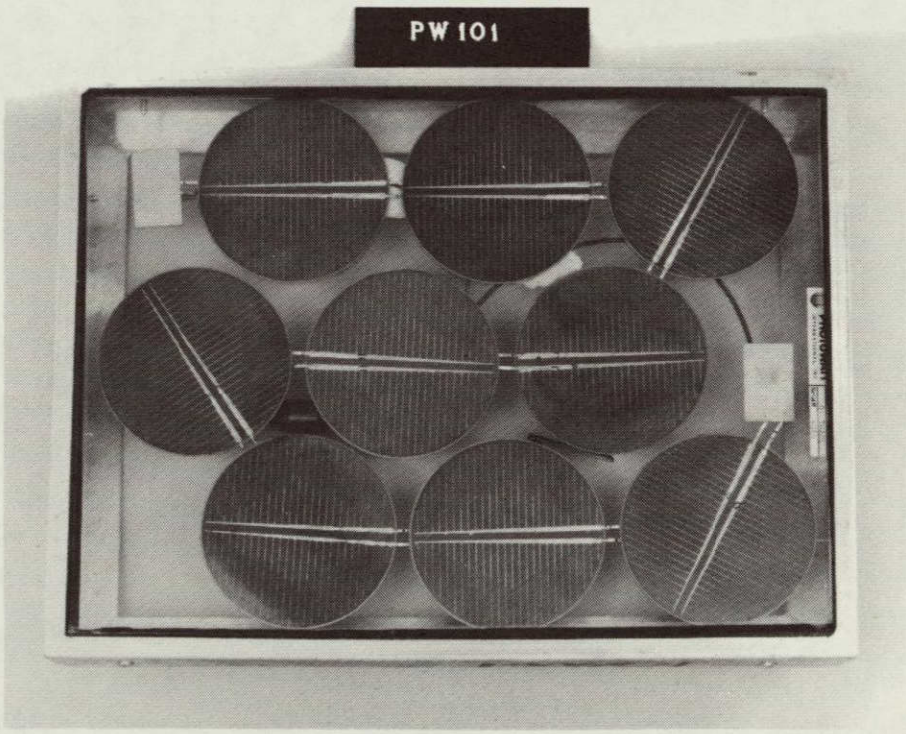

Type XI

TYPE XII
PW 116 - 130

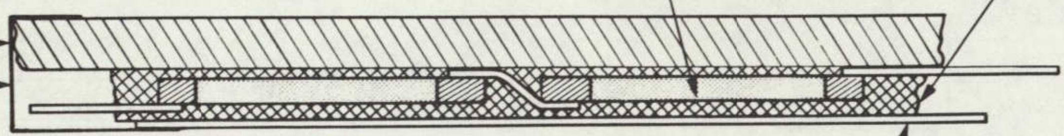

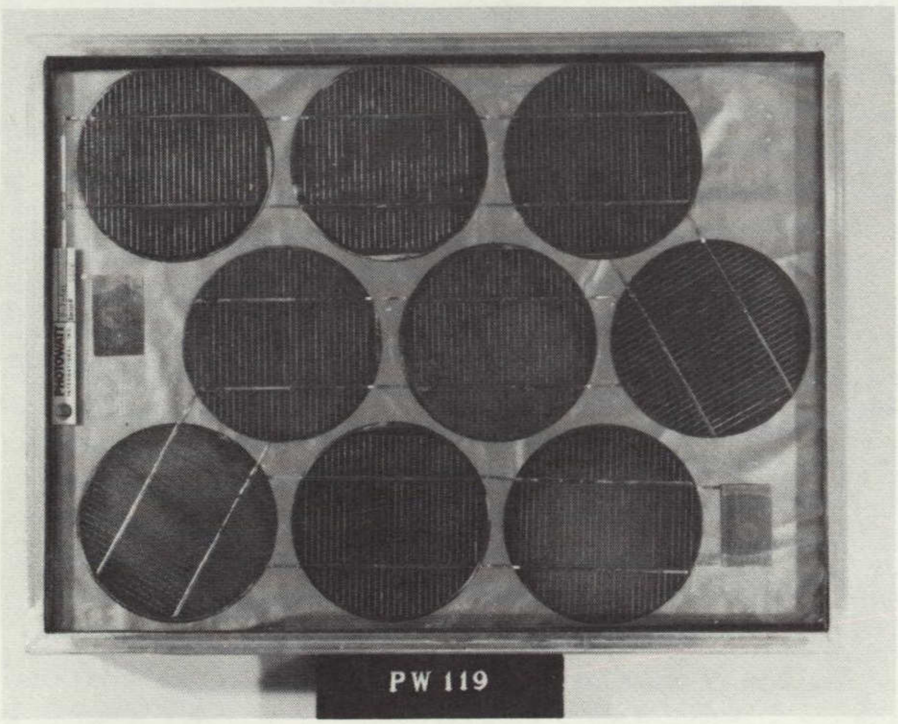

Type XII

APPENDIX C

EFFECT OF EXPOSURE ON MAXIMUM POWER OUTPUT

(Minimodules and Submodules Tested in the JPL Large-Area Pulsed Solar Simulator)

Table C-1. Effect of Exposure on Maximum Power Output - Minimodules at JPL

Serial Number	Initial P_{max}, watts	Percentage of Initial Maximum Power Retained (Before/After Cleaning)						
	Days of exposure:	30	63	94	180	309	565	718
	Date removed for test:	8-6-80	9-8-80	10-23-80	1-21-81	6-4-81	3-4-82	8-20-82
TYPE I								
DE101	7.12	95/98	96/98	97/99	97/98	93/97	96/100	93/96
DE102	6.30	87/74	67/69	(1)	-	-	-	-
DE103	6.33	93/77	30/31	(2)	-	-	-	-
TYPE III								
DE131	7.08	95/98	94/97	95/99	97/98	93/97	98/99	87/97
DE132	6.28	95/98	95/98	94/99	97/98	93/97	98/100	87/96
DE133	6.80	96/100	97/101	97/101	99/100	95/100	101/102	91/100
TYPE IV								
MB110	8.85	95/98	94/98	91/98	95/99	93/99	100/102	85/97
MB111	8.88	96/98	94/95	92/98	96/99	93/99	98/101	83/97
MB112	8.50	96/100	96/103	93/100	98/100	95/100	98/104	87/100
TYPE V								
DE117	6.77	97/101	98/100	96/88	98/99	96/98	98/100	92/97
DE118	6.16	82/98	95/97	93/97	95/96	93/95	95/97	89/95
DE119	6.38	98/102	99/102	98/102	100/105	97/100	100/101	93/100
TYPE VI								
CE110	10.96	96/100	97/100	94/100	98/99	96/100	101/102	90/100
CE111	10.33	96/97	96/100	94/99	98/100	96/99	100/102	87/99
CE113	10.56	95/99	95/98	94/99	97/97	95/97	98/100	87/97
TYPE VII								
CE123	10.52	96/100	96/99	95/99	97/98	94/98	99/100	85/98
CE124	10.11	93/97	94/97	93/96	95/96	93/96	97/99	84/96
CE125	10.79	94/98	95/97	94/98	97/97	94/96	98/98	85/96

(1) One cracked cell - removed from test.
(2) Three cracked cells - removed from test.

Table C-1. Effect of Exposure on Maximum Power Output - Minimodules at JPL (cont'd)

Serial Number	Initial P_{max}, watts	Days of exposure: / Date removed for test:	Percentage of Initial Maximum Power Retained (Before/After Cleaning) 30 / 8-6-80	63 / 9-8-80	94 / 10-23-80	180 / 1-21-81	309 / 6-4-81	565 / 3-4-82	718 / 8-20-82
TYPE VIII									
CE134	11.12		95/99	94/99	94/98	97/98	94/97	99/100	82/98
CE135	10.36		95/99	94/99	94/98	97/98	94/98	99/101	84/98
CE136	11.09		95/99	94/99	95/99	97/98	95/98	99/100	83/98
TYPE IX									
SE101	9.83		98/100	96/99	93/98	96/99	96/99	100/101	92/97
SE102	10.01		98/101	98/100	95/99	96/100	97/100	100/102	92/97
TYPE X									
GE102	9.48		97/100	90/99	94/101	95/97	95/97	100/101	92/101

Serial Number	Initial P_{max} watts	Days of exposure: / Date removed for test:	Percentage of Initial Maximum Power Retained (Before/After Cleaning) 42 / 6-4-81	121 / 9-8-81	294 / 3-4-82	447 / 8-20-82
TYPE XI						
PW104	5.326		95/98	97/98	101/102	97/99
PW105	6.345		94/98	91/99	98/98	94/95
PW106	6.166		98/99	97/99	103/103	98/100
TYPE XII						
PW119	6.076		96/99	96/98	102/102	97/99
PW120	5.571		96/98	95/99	101/101	95/96
PW121	7.477		95/98	94/96	100/101	94/95

Table C-2. Effect of Exposure on Maximum Power Output - Minimodules at Goldstone

Serial Number	Initial P_{max}, watts	Percentage of Initial Maximum Power Retained (Before/After Cleaning) — Days of exposure: / Date removed for test: 33 / 11-5-80	102 / 1-13-81	138 / 2-24-81	263 / 7-9-81	473 / 2-10-82	503 / 3-26-82	649 / 9-1-82
TYPE I								
DE104	6.21	96/97	92/93	92/94	92/88	25/(1)	-	-
DE105	6.47	80/80	78/79	45/77	80/50	44/(1)	-	-
DE106	6.39	97/97	95/96	98/98	95/95	97/97	98/98	96/95
TYPE III								
DE134	6.69	97/99	98/98	100/99	99/99	101/101	102/102	100/99
DE135	6.79	99/99	94/99	101/101	99/100	101/101	102/102	99/99
DE136	6.63	98/98	98/95	100/99	97/98	99/97	101/101	98/98
TYPE IV								
MB113	8.74	98/100	97/100	101/100	98/99	102/102	103/102	99/99
MB114	8.70	97/98	98/98	99/98	96/97	99/99	100/100	97/97
MB115	8.70	97/100	99/100	94/94	98/98	101/102	101/101	98/99
TYPE V								
DE120	6.29	96/97	95/95	96/96	94/95	96/96	96/96	94/93
DE121	6.10	99/100	98/99	100/97	97/98	99/99	101/100	97/93
DE122	6.44	101/102	100/101	102/99	98/100	102/102	102/102	100/100
TYPE VI								
CE105	11.33	96/97	96/97	97/98	95/96	99/99	99/99	96/97
CE106	10.08	106/97	96/94	97/97	95/95	99/97	98/98	96/95
CE107	10.43	97/98	95/97	98/97	96/97	99/99	100/100	97/98

(1) Blown off rack during exposure period - removed for failure analysis.

Table C-2. Effect of Exposure on Maximum Power Output - Minimodules at Goldstone (cont'd)

Serial Number	Initial P_{max}, watts	Percentage of Initial Maximum Power Retained (Before/After Cleaning)							
		Days of exposure:	33	102	138	263	473	503	649
		Date removed for test:	11-5-80	1-13-81	2-24-81	7-9-81	2-10-82	3-26-82	9-1-82
TYPE VII									
CE120	11.32		94/96	94/95	96/95	94/95	97/96	97/98	95/95
CE121	10.77		96/97	95/96	97/97	94/96	99/98	98/99	96/96
CE122	10.83		95/97	95/96	96/96	94/95	98/98	98/98	95/95
TYPE VIII									
CE140	10.22		96/99	97/97	98/98	97/97	100/100	100/100	97/97
CE141	9.79		97/98	96/99	97/98	95/97	100/98	99/99	97/97
CE142	10.57		97/98	94/96	96/98	96/97	99/99	99/100	97/97
TYPE X									
GE103	9.96		98/98	96/97	97/97	96/96	99/99	100/100	98/97

Serial Number	Initial P_{max}, watts	Percentage of Initial Maximum Power Retained (Before/After Cleaning)						
		Days of exposure:	29	77	110	279	309	455
		Date removed for test:	5-7-81	7-9-81	8-19-81	2-10-82	3-26-82	9-1-82
TYPE IX								
SE109	9.47		100/98	97/98	97/97	100/100	101/102	98/98
SE110	9.69		94/94	91/86	93/95	83/86	91/96	87/97
SE120	9.75		90/93	94/96	85/84	52/(2)	-	-
TYPE XI								
PW101	5.756		97/99	96/98	98/99	101/101	101/102	98/98
PW102	6.163		96/99	96/97	97/98	100/101	102/101	97/97
PW103	5.293		97/100	98/98	97/99	101/100	102/101	97/97
TYPE XII								
PW116	5.749		97/98	97/98	98/99	101/101	101/101	96/96
PW117	3.588		94/98	96/97	95/98	97/99	99/98	91/92
PW118	5.778		97/99	97/98	98/99	100/101	101/101	96/97

(2) Removed for failure analysis.

Table C-3. Effect of Exposure on Maximum Power Output - Minimodules at Pt. Vicente

Serial Number	Initial P_{max}, watts	Percentage of Initial Maximum Power Retained (Before/After Cleaning) — Days of exposure: 48; Date removed for test: 12-8-80	90 1-23-81	126 3-6-81	126+ Storage(1)	21(1) 12-30-81	106(1) 4-8-82	165(1) 6-17-82
TYPE I								
DE107	6.32	98/89	(2)	93/93	82	95	86/87	84/85
DE108	6.75	101/101	(3)	-	-	-	-	-
DE109	6.44	100/100	97/97	98/97	96	98	98/98	94/96
TYPE III								
DE137	6.27	100/102	100/100	101/100	100	104	101/101	98/100
DE138	6.37	100/100	98/99	98/98	99	101	99/99	91/94
DE139	6.62	99/99	(4)	-	-	-	-	-
TYPE IV								
MB116	8.75	102/102	101/101	101/102	104	105	103/104	98/101
MB117	8.89	99/100	100/100	98/100	102	104	101/103	96/100
MB118	8.65	101/101	101/101	100/101	103	105	102/103	98/101
TYPE V								
DE123	5.96	99/99	97/105	98/97	97	99	97/98	95/97
DE124	5.63	100/100	98/99	99/92	96	114	87/88	85/85
DE125	6.05	100/100	98/98	97/97	98	106	97/98	94/96
TYPE VI								
CE101	11.15	98/98	95/96	96/96	100	101	97/99	94/97
CE102	10.24	99/99	97/97	97/98	101	102	99/100	96/99
CE104	10.04	99/99	97/96	96/97	100	100	98/99	95/98

(1) After previous exposure followed by 269 days of storage in the dark.
(2) Removed for failure analysis on 12-8-80.
(3) Stolen sometime between 1-12-81 and 1-23-81.
(4) Electrical connection broken in removing from rack.

Table C-3. Effect of Exposure on Maximum Power Output - Minimodules at Pt. Vicente (cont'd)

Serial Number	Initial P_{max}, watts	Percentage of Initial Maximum Power Retained (Before/After Cleaning) — Days of exposure: / Date removed for test: 48 / 12-8-80	90 / 1-23-81	126 / 3-6-81	126+ / Storage[1]	21[1] / 12-30-81	106[1] / 4-8-82	165[1] / 6-17-82
TYPE VII								
CE117	11.17	97/98	95/95	95/95	99	101	97/99	93/96
CE118	10.80	97/97	95/95	95/95	99	101	97/99	94/96
CE119	10.26	99/98	95/96	96/96	100	102	98/99	95/97
TYPE VIII								
CE137	10.67	99/99	96/97	96/97	100	100	99/99	(5)
CE138	10.14	98/98	95/96	95/95	95	102	97/99	(5)
CE139	10.47	99/99	96/96	97/96	101	102	98/100	(5)
TYPE IX								
SE105	1.004	-	-	-	100	102	102/99	96/97
SE106	9.361	-	-	-	99	102	96/97	95/95
SE121	6.882	-	-	-	100	102	98/98	93/94
TYPE X								
GE104	9.99	99/100	(6)	-	-	-	-	-
TYPE XI								
PW112	6.696	-	-	-	103	103	101/103	97/98
PW113	5.893	-	-	-	102	103	101/103	96/98
PW114	5.194	-	-	-	102	103	102/102	97/98
TYPE XII								
PW127	7.705	-	-	-	102	102	101/100	95/97
PW128	6.086	-	-	-	102	101	101/100	95/97
PW129	7.326	-	-	-	101	101	101/100	96/96

(5) These three modules stolen between 4-20-82 and 6-17-82.
(6) Stolen sometime between 1-12-81 and 1-23-81.

Table C-4. Effect of Exposure on Maximum Power Output - Submodules at JPL

Serial Number	Initial P_{max}, watts		Percentage of Initial Maximum Power Retained (Before/After Cleaning)	
		Days of exposure:	201	353
		Date removed for test:	2-3-81	7-20-81
TYPE I				
DE416	1.225		96/95	88/94
DE417	1.144		95/95	84/88
DE418	1.098		97/97	89/95
DE419	1.189		59/81	(1)
DE420	1.127		87/87	50/55
DE421	1.151		94/96	83/86
DE422	1.114		96/98	90/94
DE423	1.203		96/97	89/93
DE424	1.153		97/98	91/90
DE425	1.208		91/92	86/80
DE426	1.240		52/(1)	-
DE427	1.101		95/96	77/78
DE428	1.098		96/98	90/95
DE429	1.119		96/98	88/93
DE430	1.187		93/93	(1)
DE431	1.121		101/98	91/95
DE432	1.215		91/87	55/17
DE433	1.281		84/36	(1)
DE434	1.244		84/94	79/79
DE435	1.113		100/97	89/93
DE436	1.142		101/97	90/95
DE437	1.136		100/95	88/92
DE438	1.118		101/97	90/90
TYPE II				
DE516	1.225		93/94	88/91
DE517	1.206		93/95	87/92
DE518	1.442		95/96	92/94
DE519	1.639		96/97	94/95
DE520	1.638		96/97	90/95
DE521	1.292		92/93	86/90
DE522	1.267		94/92	27/68

(1) No output - removed for failure analysis.
(2) Removed for failure analysis.

Table C-4. Effect of Exposure on Maximum Power Output - Submodules at JPL (cont'd)

Serial Number	Initial P_{max}, watts	Days of exposure: / Date removed for test:	Percentage of Initial Maximum Power Retained (Before/After Cleaning) 201 / 2-3-81	353 / 7-20-81
TYPE II (cont'd)				
DE523	1.382		92/94	80/84
DE524	1.183		93/93	88/93
DE525	1.507		91/92	109/91
DE526	1.156		91/91	86/90
DE527	1.279		90/89	42/82
DE528	1.258		94/94	47/90
DE529	1.201		95/95	44/94
DE530	1.282		87/87	35/70
DE531	0.833		139/154	81/153
DE532	1.306		96/97	50/95
DE533	1.377		94/96	49/95
DE534	1.084		90/90	35/74
DE535	1.260		93/95	48/91
DE536	1.426		93/95	49/93
DE537	1.395		82/81	32/54
DE538	1.261		91/93	46/90
TYPE III				
DE316	1.096		101/101	94/98
DE317	1.083		101/102	93/100
DE318	1.109		101/101	93/100
DE319	1.096		99/100	93/98
DE320	1.081		99/101	92/98
DE321	1.154		99/100	92/99
DE322	1.142		101/101	94/100
DE323	1.127		101/101	94/99
DE324	1.069		101/101	94/100
DE325	1.086		99/99	89/97
DE326	1.092		99/101	94/99
DE327	1.102		100/99	93/97
DE328	1.157		99/99	91/97
DE329	1.164		100/100	95/97
DE330	1.152		101/100	94/99
DE331	1.140		101/100	95/98
DE332	1.118		99/99	96/99
DE333	1.110		97/98	93/94
DE334	0.812		130/130	126/127
DE335	1.112		99/99	96/97
DE336	1.086		105/107	104/107
DE337	1.131		99/100	97/101
DE338	1.148		99/98	95/95

ORIGINAL PAGE IS OF POOR QUALITY

Table C-4. Effect of Exposure on Maximum Power Output - Submodules at JPL (cont'd)

Serial Number	Initial P_{max}, watts		Percentage of Initial Maximum Power Retained (Before/After Cleaning)	
		Days of exposure:	201	353
		Date removed for test:	2-3-81	7-20-81
TYPE V				
DE216	1.184		100/101	92/99
DE217	1.039		100/103	91/101
DE218	1.116		99/102	90/99
DE219	1.112		98/100	98/97
DE220	1.146		100/100	90/98
DE221	1.026		99/101	91/99
DE222	1.134		98/99	89/98
DE223	1.113		98/100	89/98
DE224	1.107		99/100	90/99
DE225	1.103		99/100	90/99
DE226	1.074		99/101	91/100
DE227	1.131		98/99	89/98
DE228	1.147		99/100	90/99
DE229	0.981		99/100	92/98
DE230	1.117		100/101	92/99
DE231	1.098		98/100	90/99
DE232	1.083		99/100	91/98
DE233	1.146		100/101	91/99
DE234	1.147		98/100	90/98
DE235	1.118		100/101	92/99
DE236	1.092		99/102	92/100
DE237	1.140		98/102	94/101
DE238	1.113		100/101	91/99

Table C-5. Effect of Exposure on Maximum Power Output - Submodules at Goldstone

Serial Number	Initial P_{max}, watts	Days of exposure: / Date removed for test:	35 / 3-17-81	78 / 5-7-81	112 / 6-23-81
		Percentage of Initial Maximum Power Retained (Before/After Cleaning)			
TYPE I					
DE443	1.132		97/97	96/96	93/96
DE444	1.232		94/95	93/94	90/94
DE445	1.069		98/98	98/98	95/97
DE446	1.180		95/94	94/93	91/93
DE447	1.116		77/94	94/94	91/93
DE448	1.111		97/97	97/97	95/97
DE449	1.098		94/94	94/93	91/94
DE450	1.104		96/95	95/93	92/95
DE451	1.143		95/95	95/94	93/95
DE452	1.092		94/94	95/93	94/94
DE453	1.148		95/95	94/93	93/93
DE454	1.153		93/93	88/87	87/88
DE455	1.109		94/94	94/93	93/93
DE456	1.047		96/95	96/95	94/95
DE457	1.089		94/95	95/95	94/95
DE458	1.112		95/95	95/95	94/95
DE459	1.123		92/92	84/84	87/86
DE460	1.185		94/94	94/93	93/92
DE461	1.136		93/92	90/90	95/90
DE462	1.107		97/95	95/95	94/95
TYPE II					
DE544	1.139		97/93	93/95	93/93
DE545	1.223		98/95	93/96	94/95
DE546	1.298		96/95	93/94	92/93
DE547	1.240		96/95	91/93	90/92
DE548	1.580		98/97	95/97	94/95
DE549	1.627		98/98	95/96	95/96
DE550	1.285		95/95	92/93	92/75
DE551	1.295		96/94	92/93	91/92
DE552	1.238		97/95	93/95	92/94
DE553	1.295		97/96	92/95	93/93
DE554	1.560		96/91	82/83	96/92
DE555	1.482		101/99	97/99	96/98
DE556	1.508		80/*	-	-
DE557	1.535		98/99	97/98	96/97
DE558	1.292		97/98	96/97	95/96
DE559	1.242		97/98	95/97	96/96

*No output - removed for failure analysis.

ORIGINAL PAGE IS
OF POOR QUALITY

Table C-5. Effect of Exposure on Maximum Power Output - Submodules at Goldstone (cont'd)

Serial Number	Initial P_{max}, watts	Percentage of Initial Maximum Power Retained (Before/After Cleaning) Days of exposure: 35 Date removed for test: 3-17-81	78 5-7-81	112 6-23-81
TYPE II (cont'd)				
DE560	1.500	98/98	96/99	98/98
DE561	1.399	97/97	95/99	96/97
DE562	1.223	96/97	93/96	94/95
DE563	1.413	105/105	103/105	104/104
DE564	1.442	99/99	97/99	98/98
TYPE III				
DE343	1.125	97/98	95/97	94/95
DE344	1.066	98/99	97/98	96/96
DE345	1.137	98/99	97/98	96/96
DE346	1.172	98/99	98/98	96/97
DE347	1.134	98/99	97/99	96/97
DE348	1.138	97/97	95/97	94/95
DE349	1.123	98/99	98/99	95/96
DE350	1.099	100/97	95/97	94/95
DE351	1.140	97/98	97/98	95/96
DE352	1.117	98/99	97/99	96/97
DE353	1.148	97/98	95/97	94/95
DE354	1.154	98/98	96/97	95/96
DE355	1.131	98/98	97/98	95/96
DE356	1.118	97/97	95/96	94/95
DE357	1.137	99/98	97/98	96/97
DE358	1.145	97/97	97/97	94/94
DE359	1.168	99/98	98/98	96/97
DE360	1.152	99/96	96/97	94/97
DE361	1.167	100/98	99/100	97/99
DE362	1.133	96/95	95/95	93/94
DE363	1.062	98/97	96/97	95/96
TYPE V				
DE244	1.018	100/99	98/99	97/97
DE245	1.123	100/98	97/98	96/98
DE246	0.997	101/100	100/99	97/98
DE247	1.230	101/101	100/100	98/100
DE248	1.132	98/98	97/98	96/98
DE249	1.108	102/101	101/101	99/101

Table C-5. Effect of Exposure on Maximum Power Output - Submodules at Goldstone (cont'd)

Serial Number	Initial P_{max} watts	Percentage of Initial Maximum Power Retained (Before/After Cleaning) Days of exposure: 35 Date removed for test: 3-17-81	78 5-7-81	112 6-23-81
TYPE V (cont'd)				
DE250	1.120	101/101	100/101	99/100
DE251	1.174	100/99	97/99	97/98
DE252	1.123	100/101	99/99	97/98
DE253	1.066	100/101	99/99	97/99
DE254	1.055	101/101	99/100	98/99
DE255	1.095	102/102	99/100	97/99
DE256	1.089	100/100	100/99	99/99
DE257	1.105	100/100	97/99	98/98
DE258	1.056	99/99	97/98	96/97
DE259	1.182	102/102	101/102	100/100
DE260	1.067	99/100	96/99	98/98
DE261	1.056	98/100	97/98	97/97
DE262	1.147	101/102	99/100	98/99
DE263	1.115	101/102	99/100	99/98
DE264	1.105	98/100	97/98	96/96

Table C-6. Effect of Exposure on Maximum Power Output - Submodules at Pt. Vicente

Serial Number	Initial P_{max}, watts	Percentage of Initial Maximum Power Retained (Before/After Cleaning) — Days of exposure: 28+Storage*; Date removed for test: 3-14-81
TYPE I		
DE463	1.099	95
DE464	1.130	97
DE465	1.153	96
DE466	1.098	97
DE467	1.171	93
DE468	1.163	96
DE469	1.130	96
DE470	1.141	94
DE471	1.194	94
DE472	1.135	96
DE473	1.126	95
DE474	1.099	97
DE475	1.124	97
DE476	1.168	95
DE477	1.196	93
DE478	1.079	95
DE479	1.143	96
DE480	1.125	95
DE481	1.123	96
DE482	1.165	94
DE483	1.137	96
DE484	1.106	95
DE485	1.087	96
TYPE II		
DE565	1.531	97
DE566	1.491	99
DE567	1.345	98
DE568	1.593	95
DE569	1.276	95
DE570	1.550	97
DE571	1.533	100
DE572	1.315	97
DE573	1.534	97
DE574	1.249	98
DE575	1.417	96

*After 28 days exposure followed by 269 days of storage in the dark.

Table C-6. Effect of Exposure on Maximum Power Output - Submodules at Pt. Vicente (cont'd)

Serial Number	Initial P_{max}, watts	Percentage of Initial Maximum Power Retained (Before/After Cleaning) — Days of exposure: 28+Storage*; Date removed for test: 3-14-81
TYPE II (cont'd)		
DE576	0.664	97
DE577	1.310	95
DE578	1.339	96
DE579	1.209	97
DE580	1.227	100
DE581	1.369	99
DE582	1.134	100
DE583	1.374	94
DE584	1.394	100
DE585	1.408	99
TYPE III		
DE364	1.111	97
DE365	1.145	99
DE366	1.151	97
DE367	1.093	97
DE368	1.153	97
DE369	1.094	98
DE370	1.146	97
DE371	1.125	99
DE372	1.125	97
DE373	1.155	96
DE374	1.087	99
DE375	1.168	99
DE376	1.187	99
DE377	1.170	99
DE378	1.204	99
DE379	1.181	95
DE380	1.168	99
DE381	1.135	97
DE382	1.177	97
DE383	1.118	98

Table C-6. Effect of Exposure on Maximum Power Output - Submodules at Pt. Vicente (cont'd)

Serial Number	Initial P_{max}, watts	Percentage of Initial Maximum Power Retained (Before/After Cleaning) Days of exposure: 28+Storage* Date removed for test: 3-14-81
TYPE V		
DE265	1.273	99
DE266	1.087	98
DE267	1.039	99
DE268	1.139	99
DE269	1.129	98
DE270	1.096	99
DE271	1.057	97
DE272	1.130	97
DE273	1.117	99
DE274	1.140	101
DE275	1.085	99
DE276	1.081	98
DE277	1.113	98
DE278	1.193	97
DE279	1.122	96
DE280	1.191	98
DE281	1.071	97
DE282	1.061	96
DE283	1.093	96
DE284	1.152	98
DE285	1.181	98